Vol. 682: 169–189, 2022
https://doi.org/10.3354/meps13925

MARINE ECOLOGY PROGRESS SERIES
Mar Ecol Prog Ser

Published January 20

Offshore snapper and shark distributions are predicted by prey and area of nearby estuarine environments in the Gulf of Mexico, USA

Bradley A. Pickens[1,4,*], J. Christopher Taylor[2], Matthew D. Campbell[3], William B. Driggers III[3]

[1]CSS-Inc. (under contract from NOAA National Centers for Coastal Ocean Science), Fairfax, Virginia 22030, USA
[2]NOAA National Centers for Coastal Ocean Science, Beaufort, North Carolina 28516, USA
[3]National Marine Fisheries Service, Southeast Fisheries Science Center, Mississippi Laboratories, Pascagoula, Mississippi 39567, USA
[4]*Present address:* US Fish and Wildlife Service, 11510 American Holly Dr., Laurel, Maryland 20708, USA

ABSTRACT: Seascape ecology has demonstrated that marine fishes are associated with multiscale habitat characteristics; however, most species distribution models focus on only a few predictors (e.g. depth, temperature), and this limits knowledge of essential fish habitat characteristics. Our objectives were to (1) determine habitat associations of offshore predatory marine fishes using a comprehensive suite of predictors, including area of nearby estuarine environments, (2) assess variable influence, and (3) model the spatial distribution of selected fishes in the families Carcharhinidae and Lutjanidae. We hypothesized that the concept of coastal outwelling would be evidenced by species associations with areas of nearby estuarine environments, and prey abundance would correlate with predator distributions. Species distribution models were developed for 2 snapper and 3 shark species in the northern Gulf of Mexico, USA. We used 34 multiscale predictors to evaluate how fish probability of presence or catch per unit effort (CPUE) were associated with oceanography, geography, substrate, area of nearby wetlands and estuaries, and prey abundance. Boosted regression trees, a machine-learning technique, modeled the most influential variables and predicted distributions. Model validation showed an overall accuracy of 79–86%, and CPUE models explained >40% of model deviance. Oceanographic variables, particularly mixed layer depth, were most influential and most frequently selected. As hypothesized, predatory fish distributions were predicted by prey abundances, and shark distributions were predicted by area of nearby coastal wetlands and estuaries. Our findings suggest that spatial models can provide novel insights into prey associations and linkages of marine species with nearby wetlands and estuaries.

KEY WORDS: Species distribution model · Habitat use · Prey · Wetlands · Outwelling hypothesis · Carcharhinidae · Lutjanidae · Mixed layer depth

1. INTRODUCTION

Knowledge of species-specific spatial distributions is fundamental to meeting conservation and management objectives (Elith & Leathwick 2009, Guisan et al. 2013). In the marine environment, species distribution models (SDMs) have proliferated in the last decade (Robinson et al. 2017, Melo-Merino et al. 2020) as technology, availability of spatial data, and computation capacity have rapidly improved. SDMs can simultaneously illuminate species–habitat relationships as well as map the spatial patterns of spe-

*Corresponding author: bradley_pickens@fws.gov

Publisher: Inter-Research · www.int-res.com

cies distributions. Although SDMs are based on correlative models, the ability to quantify the effect of multiscale predictors has led to a new field of seascape ecology (Pittman et al. 2011). Seascape analyses have confirmed expectations that marine fish distributions are dynamic over multiple spatial and temporal scales (Mannocci et al. 2017), including broad-scale effects such as offshore reef fish distribution being associated with distant mangrove and seagrass habitats (Olds et al. 2012, Martin et al. 2015). For these reasons, determining the most relevant spatial scales that link patterns and processes of marine systems has been identified as a research priority in seascape ecology (Pittman et al. 2021).

Depth and sea surface temperature (SST) are the most frequently utilized variables when examining the spatial distributions of marine organisms (Melo-Merino et al. 2020). These variables are often correlated, and temperature can define the extent of species distributions based on an optimization of physiological conditions for organisms (Kearney & Porter 2009). In contrast, variables such as ocean productivity, salinity, temperature gradients or fronts, and ocean currents influence species distribution at a finer scale often termed the mesoscale (Hobday & Hartog 2014). Prey distributions and substrate type may further characterize fine-scale habitat influences on species distributions. At a fine scale, depth and temperature are likely indirectly related to fish distribution. For example, depth may correlate with fish distribution because of varying salinity, light availability, phytoplankton concentration, prey distribution, or other variables. Possible correlates with temperature include productivity gradients or upwelling, which can modulate prey distribution. More direct predictors, including food availability, that are directly associated with species-specific resource needs are considered among the most robust variables, yet are challenging to quantify (Austin 2002). Nonetheless, the identification of direct habitat associations has the potential to provide insights into habitat requirements of species. More specifically, US policy protects 'Essential Fish Habitat,' defined as the waters and substrates required for a species to spawn, breed, feed, or grow to maturity (US Sustainable Fisheries Act of 1996, Public Law 104-297). Modeling studies have identified the ecological requirements for marine fishes in this management context (Moore et al. 2016, Pennino et al. 2016), and while predator–prey overlap is expected, few studies have tested the predictive capacity of these biological predictor variables particularly at ocean-basin scales (Robinson et al. 2011, Pickens et al. 2021c).

Productivity of marine environments is often measured using chlorophyll *a* (Melo-Merino et al. 2020), upwelling strength (Santora et al. 2014, Marin-Enriquez et al. 2018), or oceanographic fronts (Scales et al. 2014, Queiroz et al. 2016). However, cross-system trophic interactions are likely to occur across coastal environments (Zuercher & Galloway 2019), particularly between extremely productive salt marsh–estuary systems and the oceanic environment. The original 'outwelling hypothesis' developed by Odum (1980) postulates that the high production of marsh–estuarine systems has a net export of detritus and particulate organic carbon into the coastal ocean. Subsequent studies have shown that this carbon export is not likely substantial, and Deegan et al. (2002) proposed that coastal wetlands primarily support offshore fisheries by exporting juvenile fish biomass, as salt marshes support a trophic transfer of energy from primary productivity to invertebrates and nekton; subsequently, nekton undergo ontogenetic shifts and cyclic migration that export energy to the marine environment in the form of fish biomass. For example, Deegan (1993) quantified the export of Gulf menhaden *Brevoortia patronus* from estuaries to offshore waters and found that the export accounted for 5–10% of inshore primary productivity measured as annual carbon, biomass, and kilocalories exported. Similarly, estuarine-dependent brown shrimp *Penaeus aztecus* have been identified as a key component of marine fish food webs in Europe (Poiesz et al. 2020), and mangroves are thought to support offshore fisheries in Asia (Chong 2007). The relationship between estuarine wetlands and marine predators has rarely been tested or demonstrated. Overall, few studies have examined whether marine fish distributions are associated with predictors depicting prey species abundance or adjacent estuarine wetlands (Pickens et al. 2021c). In particular, understanding spatial linkages between inshore and offshore habitats used by marine species has important implications for coastal ocean management that seeks to minimize impacts to fisheries habitats from human uses.

Because of the prominence and variability of coastal environments in the northern Gulf of Mexico (nGoM), and availability of fishery-independent data, it is an ideal setting to test predator–prey and estuarine–wetland relationships with predators like snappers (Lutjanidae) and coastal sharks (Carcharhinidae). Estuarine waters, particularly in conjunction with coastal wetlands, in the nGoM provide habitat for estuarine-dependent early life stages of marine fishes and are fundamental habitat for abundant prey resources such as forage fish, shrimp, and crabs

(Spies et al. 2016). Food webs in the nGoM show common linkages among penaeid shrimp, menhaden (*Brevoortia* spp.), squid, snapper, and sharks (Tarnecki et al. 2016). In particular, the amount of Gulf menhaden consumption is projected to have major effects on the biomass of higher trophic level fisheries (Robinson et al. 2015, Geers et al. 2016).

The objectives of our study were to: (1) develop species distribution models for 2 snapper and 3 shark species with diverse life history requirements; (2) determine habitat relationships using a broad suite of multiscale predictor variables, including prey abundance, area of nearby estuaries and wetlands, substrate type and complexity, and oceanographic characteristics; and (3) examine the influence of predictors across these models. We hypothesized that prey distribution and the area of nearby estuarine habitats would be important predictors of the spatial distribution of predatory species in the marine environment.

2. MATERIALS AND METHODS

2.1. Study area

The study area spanned the nGoM from Texas to Florida, USA. The landward boundary began with federally managed waters (5.6 km from the shore of Louisiana, Mississippi, and Alabama; 16.7 km from the shore of Texas and Florida) through the 50 m depth contour. Only waters ≤50 m in depth were included because our focus was on examining potential sand-dredging impacts to fisheries habitat (see Kim et al. 2008, Drabble 2012, Hwang et al. 2013). Benthic substrate of the study area consists of unconsolidated sediments ranging from mud to gravel with natural patches of hardbottom reefs scattered throughout but primarily associated with the West Florida Shelf and the shelf edge break (Rezak et al. 1985). Additionally, since the 1950s, >20 000 artificial reefs and >4000 oil and gas platforms have been installed in the GoM, with approximately 3900 oil and gas platforms remaining (Shipp & Bortone 2009). These structures are common in the western part of the study area and provide complex substrate to fishes.

2.2. Biological data

We modeled the distribution of juvenile red snapper *Lutjanus campechanus* (ages 0 and 1), lane snapper *L. synagris* (ages 0 and 1), blacktip sharks *Carcharhinus limbatus*, spinner sharks *C. brevipinna*, and Atlantic sharpnose sharks *Rhizoprionodon terraenovae*. These species were selected based on their designation as federally managed species with designated Essential Fish Habitat in shallow waters, data availability, economic importance, known prey associations (e.g. Gulf menhaden), and their potential association with unconsolidated sediments, sand shoals, and substrate complexity. We used fishery-independent data collected from 2003 to 2017 to evaluate spatial distributions of each species. Shark catch per unit effort (CPUE) data were collected during annual bottom longline surveys conducted by the National Marine Fisheries Service, Mississippi Laboratories, and conducted annually throughout the nGoM from July through September. In addition, we used data from the Congressional Supplemental Sampling Program, an extensive bottom longline survey that occurred from 7 April through 25 October of 2011. Both bottom longline surveys were conducted using standardized methods described in detail by Driggers et al. (2012). Briefly, surveys were conducted using random-stratified survey designs throughout the nGoM. All bottom longline surveys deployed 1.85 km of mainline and 100 gangions with a 15/0 circle hook baited with Atlantic mackerel *Scomber scombrus*. Gear soak times were targeted to be 1 h; however, in some cases, longline sets were shorter or longer in duration than planned due to unforeseen issues (e.g. mechanical failure, vessel traffic, weather). As a result, data from longline sets with effort outside of the 37–107 min range were excluded (<0.2% of the dataset). Seven longline sets used <80 hooks and were removed (<0.5% of dataset); data from longline sets with >85 gangions deployed were retained for analyses, and the remaining surveys had 86–104 hooks per longline set. We used presence/absence data for blacktip and spinner sharks because of their relatively low frequency of capture in the study area; for the more commonly captured Atlantic sharpnose shark, CPUE was calculated as:

$$\mathrm{CPUE} = \left(\frac{c}{h \cdot t}\right) \cdot 60 \cdot 100 \quad (1)$$

where c is the number of Atlantic sharpnose sharks captured, h is the number of hooks deployed, and t is the soak time in minutes. The multipliers 60 min and 100 hooks were used to standardize CPUE data as number of Atlantic sharpnose sharks caught per 100 hook hours. Prior to analyses, generalized additive models (GAMs) (knots = 3) were used to test the association of survey length (km) and duration (min) on species occurrence and CPUE to evaluate if associations were minimal. Given that all tests showed

that <2% of the deviance was explained by these factors, we used CPUE and occurrence data without correction.

To evaluate juvenile red and lane snapper spatial distributions, we used trawl surveys conducted as part of the Southeast Area Monitoring and Assessment Program (SEAMAP). The SEAMAP trawl surveys are conducted annually across the continental shelf of the nGoM during summer (June–August) and autumn months (October–December). With the exception of minor changes in research design implemented in 2008, the SEAMAP trawl survey has used standardized gear, protocols, and a random stratified sampling design since 1987 (Craig & Crowder 2005, Rester 2017). The SEAMAP trawl survey deploys a 12.8 m shrimp trawl with a with a mesh size of 4.1 cm stretched at the codend. In some cases when the biological catch exceeded 22.7 kg, only a subset of the snappers were counted and measured. In these cases, we projected the full trawl catch based on extrapolation of the sub-sample, and we assumed that this extrapolation applied to each age group equally. Trawl surveys targeted a 30 min duration. Extremely long or short trawl survey lengths were removed, and subsequently data from trawls ranging from 11–52 min and 1.0–5.2 km were used in analyses. Excluded data were <15% of the trawl surveys and were often in the shallowest and deepest waters within the study area, indicating logistical challenges. Trawl survey counts were transformed to CPUE, and were calculated as fish km^{-1} surveyed. Prior to analyses, we used GAMs to test the association of trawl length and duration with CPUE and occurrence of our target species to evaluate the association. All tests showed that <2% of the deviance was explained by these effects except for a negative association with age-0 red snapper (2.7% of deviance explained) and a positive association with age-1 lane snapper (4.5% of deviance explained). Given these mixed effects, we proceeded with using CPUE and occurrence data without further correction. The centroids of trawl tows and bottom longline sets were used to depict survey locations and to link surveys to predictor variables.

Each snapper age class was expected to use different habitat because both species undergo an ontogenetic shift from soft-bottom habitats occupied by juveniles to high-relief reefs occupied during young adult stages. Therefore, analyses included red snapper age 0 (51–172 mm total length [TL]) and age 1 (173–300 mm TL) as well as lane snapper age 0 (<199 mm TL) and age 1 (≥199 mm TL) (see details in Text S1 in the Supplement at www.int-res.com/articles/suppl/m682p169_supp.pdf). We did not distinguish shark ages or sexes for analyses, but the proportion of each life stage present was estimated based on length (Text S1). Of the sexed blacktip sharks, 54% were female and 46% were male. We estimated blacktip sharks sampled were 0.002% (3 individuals) young-of-year, 65% juvenile, and 35% adult. Of the sexed Atlantic sharpnose sharks, 49% were male and 51% female, and age classes showed 2% young-of-year, 27% juvenile, and 71% adult. Of sexed spinner sharks, 49% were female and 51% were male. Spinner shark age classification showed 3% young-of-year, 43% juveniles, and 54% adults. Although shark habitat use can differ by sex, we did not separate males and females in our analysis because sample size would have been reduced, not all sharks were sexed, and Essential Fish Habitat for sharks is not defined by sex in the US.

2.3. GIS methods and environmental predictor variables

Spatial analyses of environmental data were conducted in ArcGIS 10.6 (ESRI). We developed predictor variables depicting oceanography, substrate, geography, area of nearby wetlands and estuaries, and biological characteristics (Table 1). For depth, and variables derived from bathymetry, the Coastal Relief Model (NOAA National Centers for Environmental Information 2010) was used for waters near Texas, Louisiana, Mississippi, and Alabama. Offshore of Florida, we observed bathymetric artifacts in the Coastal Relief Model that spanned tens of kilometers; therefore, these data were replaced with 50 m resolution bathymetry developed by the US Geological Survey (Robbins et al. 2007). To be consistent across the study area, these data were resampled to a 90 m resolution using bilinear interpolation. From the bathymetry data, we used the ArcGIS Benthic Terrain Modeler (Walbridge et al. 2018) to calculate slope (3 × 3 cell) and the bathymetric position index (BPI). The BPI quantifies seafloor topography with values ≥1 indicating a cell is shallower than surrounding cells and a BPI ≤–1 indicating a cell is deeper than surrounding cells. Flat areas are depicted by BPI values between –1 and 1. The BPI was calculated with an inner radius of 1 cell (90 m) and an outer radius of 71 cells (6.4 km) based on the methods of Pickens et al. (2021b), who quantified seafloor topography in the nGoM to identify sand shoals. The topographic position of each cell was compared to the average position of cells over a 6.4 km radius

Table 1. Variables developed to predict the distribution of fish species in the northern Gulf of Mexico, USA. Superscripts are seasons of data included in the analysis (sp: spring; su: summer; aut: autumn). Seasons not included were removed because of multicollinearity. CV: coefficient of variation; BPI: bathymetric position index

Variable type	Predictor variable (units)	Resolution
Oceanography	Mean depth (m)	90 m
	Mean bottom temperature (°C)^{sp,aut}	4.4 km
	Mean sea surface temperature (°C)^{sp,aut}	1.2 km
	Maximum chlorophyll *a* (mg m^{-3})	5.5 km
	Minimum bottom salinity (practical salinity scale)	4.4 km
	Mean bottom current U- and V-velocity (m s^{-1})^{sp,su,aut}	9.3 km
	Mean mixed layer depth (m)$^{sp, su}$	4.4 km
	Hypoxia (mean probability; %)	90 m
Substrate	CV of depth	90 m
	Distance to shoal (km)	90 m
	Proportion of area with shoal	90 m
	Mean sediment grain size (mm)	370 m
	Proportion of area with BPI ≥1	90 m
	Slope (degrees)	90 m
	Distance to natural reef (km)	90 m
	Distance to artificial structures (km)	90 m
	Density of artificial structures (structures km^{-2})	90 m
Geography	East or west of 88° W longitude (binary)	90 m
	Distance to shoreline (km)	90 m
Nearby estuarine environments	Area of nearby wetlands (km^2)	90 m
	Area of nearby estuaries (km^2)	90 m
Biological	Species-specific prey (counts)	90 m

because sand shoal features can be several kilometers wide (Pickens et al. 2021b).

We obtained sediment grain sizes from an interpolation of point data from the US Geological Survey (Williams et al. 2012). The extent and distribution of sand shoal geoforms were obtained from Pickens et al. (2021b). To correspond to the approximate length of trawl surveys, the ArcGIS focal statistics function was used to calculate mean depth, the coefficient of variation (CV) of depth, mean slope, mean sediment grain size, proportion of area with a BPI of ≥1, and proportion of area classified as a shoal within a 3 km radius. We used a 3 km radius because this distance corresponded to the average length of trawl surveys.

Oceanographic predictors were obtained using the Marine Geospatial Ecology Toolbox (Roberts et al. 2010) (Table 1). Although fish were counted on a singular survey day, their distribution is likely determined by variation in oceanographic conditions over weeks, months, or years. Therefore, we developed climatologies for bottom water temperature, bottom salinity, mixed layer depth (MLD), and bottom current velocity for U- and V- directions from the HYbrid Coordinate Ocean Model (HYCOM) (Chassignet et al. 2009). The HYCOM data define MLD as the depth where temperature change from the surface is ≥0.2°C. Chlorophyll *a* data were a product of the Aqua MODIS satellite 8 d composites. SST was derived from the processing of a blend of satellite measures to produce high-resolution data (JPL MUR MEaSUREs Project 2015). All oceanographic measures were averaged monthly over the period of 1 January 2003 to 31 December 2017. Monthly measures were then averaged by seasons: spring = 1 March – 31 May; summer = 1 June – 31 August; autumn = 1 September – 30 November; winter = 1 December – 28/29 February). We used remote sensing data to characterize oceanographic conditions because these measures are consistent across the sampling domain and variables represent long-term spatial patterns driven by ecological processes rather than instantaneous conditions.

Hypoxia is a chronic, seasonal issue in the nGoM (Rabalais et al. 2010). To quantify hypoxia (waters with ≤2 mg l^{-1} dissolved oxygen), we used the results of Matli et al. (2018), who modeled the annual probability of hypoxia based on multiple *in situ* monitoring programs conducted by agencies and universities. From these data, the mean probability of hypoxia for July and August of 2003–2017 was used as a predictor in our models of fish occurrence. As the data were initially points, an interpolated raster dataset was created by using ordinary, spherical kriging with calculations including 8 adjacent points. Four trawl survey points southwest of the Mississippi River Delta were in waters not included in the probability of hypoxia predictor. These points were adjacent to waters with some of the highest probabilities of hypoxia (>30%), and had been recorded as hypoxic when measured by other datasets (NOAA National Centers for Environmental Information 2019). Therefore, we estimated probability of hypoxia for these waters by extrapolating from the nearest cells of hypoxia data using the ArcGIS 'expand' tool.

We developed a distance to shore variable from the spatial boundaries of the Submerged Lands Act (Office for Coastal Management 2020), which distinguishes federal and state managed waters based on

distance from shore. The ArcGIS buffer tool was used to re-create the shore boundaries, and from those we calculated the Euclidean distance from shore. A longitudinal threshold was used to depict whether the location was east (1) or west (0) of the 88° W longitude (Mobile Bay, Alabama). The CPUE of penaeid shrimp (Montero et al. 2016, Pickens et al. 2021a) and red snapper (Dance & Rooker 2019) increase drastically west of this longitude. Shallow waters west of this longitude are dominated by riverine influences, and there is substantially more mud substrate, salinity is lower, chlorophyll *a* is higher, and artificial reefs are common. To determine if the area of nearby estuarine wetlands correlates with the distribution of fish in the marine environment, we used National Wetlands Inventory data and its classification of 'estuarine and marine wetland' (US Fish and Wildlife Service 2018). We first calculated the farthest distance from an estuarine wetland in the study area, which was 160 km. Focal statistics were then used to sum the area (km^2) of estuarine wetlands within a 160 km radius of a cell in the marine environment. Estuarine waters were defined from a digital map of fish habitat (NOAA National Marine Fisheries Service 2019), which characterized all estuaries in the nGoM. To ensure only estuarine waters were included in the dataset, waters seaward of the shoreline position were removed. Similar to area of nearby wetlands, area of estuaries within a 160 km radius of each cell in the marine environment were summed together across the study area. These novel spatial metrics quantified the area of nearby estuary and wetland environments, which inherently combines both the proximity to and the area of these environments. The advantage of this method compared to typical proximity metrics is that these novel variables distinguish locations in close proximity to small estuaries/wetlands from locations in close proximity to large estuaries/wetlands.

Natural reef locations were primarily mapped during SEAMAP reef fish video surveys and were synthesized with other sources, including available charting (Rezak et al. 1985), historical knowledge from fishermen, and bathymetric mapping (i.e. side-scan sonar and multi-beam sonar) (M. Campbell & B. Noble unpublished data). We calculated artificial structures, including artificial reefs (Office for Coastal Management 2017) and oil and gas platforms (Bureau of Safety and Environmental Enforcement Gulf of Mexico OCS Region 2014), as a point density within a 3 km radius and with the Euclidean distance to the nearest artificial structure for each location in the study area. We used a 3 km radius because this distance corresponded to the average length of trawl surveys.

Potential prey associations were tested based on prior information regarding species-specific prey items, and prey distributions were characterized by their long-term spatial patterns using datasets spanning the same time period as the predatory fish surveys. This methodology, based on prior knowledge, was characterized by Wisz et al. (2013), who outlined the most appropriate statistical techniques to test biological relationships. We identified potential predator–prey associations from the literature with an emphasis on GoM research when available. For age-0 red snapper, we identified distributions of squid (*Loligo* spp.) (Szedlmayer & Lee 2004, Wells et al. 2008), mantis shrimp (*Squilla* spp.), and penaeid shrimp (Bradley & Bryan 1975, Szedlmayer & Lee 2004) as predictors. Based on Szedlmayer & Lee (2004) and Wells et al. (2008), we used searobin (*Prionotus* spp.), largescale lizardfish *Saurida brasiliensis*, and squid as predictors of age-1 red snapper. For age-0 lane snapper, the distribution of brown and pink shrimp *Penaeus duorarum* were predictors based on an estuarine study of stomach contents (Franks & VanderKooy 2000). We did not identify prey species in the literature for age-1 lane snapper, therefore no such predictors were tested. Blacktip and spinner sharks were selected for species distribution modeling in this study in part because of their strong dependence on teleost fishes (Cortés 1999), particularly menhaden prey (Bethea et al. 2004, Barry et al. 2008, Geers et al. 2016). Menhaden distribution was used as a predictor for both species, and croaker *Micropogonias undulatus* were tested with blacktip sharks based on Barry et al. (2008) and Plumlee & Wells (2016). Atlantic sharpnose sharks have high plasticity in prey, as their diet can be composed of various amounts and species of fish and crustaceans (Cortés 1999, Drymon et al. 2012, Delorenzo et al. 2015). Harrington et al. (2016) found that juveniles had a diet composed of a high quantity of penaeid shrimp, while adults consumed a high proportion of teleost fish (Harrington et al. 2016). For predictors of Atlantic sharpnose shark CPUE, we used brown shrimp (CPUE), pink shrimp (probability of presence), and, based on Bethea et al. (2004) and Plumlee & Wells (2016), menhaden and croaker abundance.

Prey predictor variables depicting the distribution of brown shrimp and pink shrimp CPUE were acquired from previously developed SDMs (Pickens et al. 2021a). We used data from SEAMAP trawl surveys to depict relative abundance of menhaden, croaker, mantis shrimp, largescale lizardfish, and

squid. We note that the collection of menhaden via trawl surveys is not ideal because of their pelagic nature, but data were otherwise not available. Prey species count data from trawl survey locations (2003–2017) were interpolated with ordinary kriging to create a continuous surface of counts using a spherical semivariogram model. To maximize accuracy, 8 points were used for analysis within a maximum distance of 10 km. The ArcGIS expand tool was used to extrapolate prey distributions when trawl surveys were >10 km from a sampled location in the study area.

2.4. Statistical analysis

All predictor variables were examined for multicollinearity, and we removed highly correlated variables ($r > 0.80$) prior to further analyses (Table 1). In addition to environmental predictors, the hour of survey was tested as a potential predictor because time of day can affect the detectability of sharks (Driggers et al. 2012) and potentially snapper. Time of day was also a variable of interest because it has implications for survey design and future analyses. Day of year was tested as a potential predictor of shark distributions; season (summer or autumn) was tested for snapper because of potential habitat differences across time. Year was not used as an explanatory variable because our research aimed to predict a singular spatial distribution of each species that represented habitat use in the region. Therefore, we assume years of high or low CPUE, or frequency of occurrence, are representative of long-term fish distribution fluctuations. The predictor variables considered for inclusion in each fish model varied with hypothesized species–habitat relationships as follows: (1) only snappers were tested with artificial structure and natural reef predictors because these substrates are a key component of their adult habitats; (2) only shark species were tested with area of nearby wetlands, area of nearby estuaries, and chlorophyll because of potential relationships with shark prey species (e.g. menhaden); (3) blacktip and spinner sharks were the only species tested with SST because they prey on menhaden, which are pelagic. The other species are primarily demersal, so only bottom temperature was considered for them.

As visualized by Pickens et al. (2021a), data used for training and validation were subset from alternating zones along a longitudinal gradient throughout the study area. Fourcade et al. (2018) showed that random splitting of data can overstate the validation accuracy of models, and the 'block' approach we used is best at distinguishing models as being poor when they are truly poor. This also served to ensure the depth gradient was represented in training and validation datasets across the longitudinal gradient. Specifically, we reclassified a raster of longitude into zones with 23 km widths across the study area. We then alternated the delineation of training (2 zones) and validation (1 zone) to define data for training and validation.

Boosted regression trees (BRTs) were used to model species–habitat relationships with the training data, and we used these models to create predictions for the entirety of the study area. For BRTs, we developed models based on predictive performance assessed from cross-validation of out-of-bag samples during each iteration (Elith et al. 2008) rather than p-values or similar metrics. BRT analyses efficiently quantify nonlinear relationships, automatically identify interactions, and can be used with many predictors (De'ath & Fabricius 2000). The predictive power of decision trees is enhanced by boosting, which sequentially adds trees that improve the model; the results are then derived from an ensemble of hundreds of trees (De'ath 2007, Elith et al. 2008). The procedures outlined by Elith et al. (2008) were used to develop BRTs and the methods are briefly summarized here. Tree complexities of 1–5 were assessed and used learning rates that resulted in >1000 trees. For CPUE models, a Poisson log-linear model was applied using CPUE as the dependent variable. For occurrence models, we used a binomial model to predict probability of presence of a given species. To avoid overfitting, the BRT simplification procedure was used, which sequentially drops the weakest predictor, ranks predictors in order of importance, and examines the change in model deviance with each drop. The inflection point where the deviance of the model abruptly increases after a drop defines which variables remain in the model with the goal of estimating the most parsimonious model. To be consistent, we defined an inflection point as an increase of >2% of the deviance explained when dropping a single variable and ≥3% for multiple dropped variables. We quantified the influence of variables with 2 techniques. First, partial dependence plots were created by examining the effect of each variable while all others were held at their mean. To create 95% prediction intervals, we used bootstrapping with replacement to create 50 samples from the model training data. The simplified BRT model was fit to each bootstrap sample and prediction intervals were determined.

Secondly, we report relative importance of variables for each species, as suggested by Elith et al. (2008). Specifically, the formulae established by Friedman (2001) are based on the frequency that a variable is selected for splitting, weighted by the squared improvement to the model as a result of each split, and averaged over all decision tree iterations (Friedman & Meulman 2003). The relative importance of all variables within a model are scaled to sum to 100%, with higher numbers being more important. The strength of interaction effects was assessed with the Friedman's *H*-statistic (*H*-statistic), which decomposes the variance explained by the partial dependence of each variable and their interaction (Friedman & Popescu 2008). An *H*-statistic of 0 shows no interaction, and a value of 1.0 shows that all of the variance explained by the partial dependence functions is dependent on the interaction. We report and visualize *H*-statistics of ≥0.15, as these were most straightforward to interpret.

Model accuracy was assessed with multiple metrics. We developed models of CPUE for the most common species, age-0 red snapper and Atlantic sharpnose sharks. To calculate accuracy of these CPUE models, we report the percent deviance explained ([null deviance – residual deviance]/null deviance) of the cross-validation and validation tests. A Spearman rank correlation (R_s) was also computed between observations from the validation dataset and the corresponding predictions. For occurrence models of age-1 red snapper, age-0 and age-1 lane snapper, blacktip sharks, and spinner sharks, we assessed accuracy with an area under the receiver operating characteristic curve (AUC) statistic, and further accuracy metrics were derived from the error matrix, comprising the true skill statistic (Allouche et al. 2006), overall accuracy, User's accuracy (percent of predictions correctly classified), and Producer's accuracy (percent of observations correctly classified) (Story & Congalton 1986). The AUC has been commonly used to test predictive ability of SDMs (Guisan & Zimmermann 2000) and is independent of thresholds. Measures of the AUC range from 0.0 to 1.0 and were interpreted as suggested by Swets (1988) as follows: <0.50 = no discriminatory power; 0.50–0.69 = poor power; 0.70–0.89 = good power; and 0.90–1.0 = excellent discriminatory power. The true skill statistic ranges from –1 to +1 with values of 0 representing random assignment. For these metrics, species-specific presence or absence was distinguished using the maximum Kappa statistic, which quantifies the probability threshold that optimally discriminates presence and absence.

Because we anticipated hierarchical relationships of fish with predictor variables (e.g. broad oceanographic variables combined with fine-scale variables depicting substrate or depth), SDMs were predicted to a 90 m resolution raster. For data initially at a resolution of >90 m, a bilinear resampling was conducted. The statistical program R (version 3.5.1.) (R Core Team 2018) and the packages 'dismo' (version 1.1-4) and 'gbm' (version 2.1.8) were used to implement BRTs. To predict models to the study area, the R packages 'rgdal' (version 1.4-4) and 'raster' (version 2.9-5) were used. We assumed the effect of survey time of day represented a detectability effect for blacktip sharks rather than a change in distribution; therefore, we applied the model at the peak time of 02:00 h. For Atlantic sharpnose sharks, day of year was a predictor in the final model, and we predicted at the peak time of year in the model (9 April).

3. RESULTS

3.1. Overall findings

Species presence ranged from 13 to 59% of sampling stations, with CPUE models being utilized with species that were present on >30% of trawls or longline sets (Table 2). The CPUE models for age-0 red snapper and Atlantic sharpnose sharks explained >40% of the deviance in the validation data with an R_s of 0.59 and 0.60 in their respective models (Table 3). All occurrence models had an AUC value of ≥0.80 when tested with validation data, indicating the models were very good at discriminating presence and absence (Table 3). Similarly, validation results had an overall accuracy of 79–86% and had a

Table 2. Frequency of select snapper species in trawls (n = 5620) and sharks captured in bottom longline sets (n = 1506) during fisheries-independent surveys conducted from 2003 to 2017 in the Gulf of Mexico, USA. CPUE: catch per unit effort

Species	Model type	% Presence	Total count
Red snapper (age 0)	CPUE	36	23 076
Red snapper (age 1)	Occurrence	19	4753
Lane snapper (age 0)	Occurrence	26	9784
Lane snapper (age 1)	Occurrence	20	1143
Atlantic sharpnose shark	CPUE	59	8765
Blacktip shark	Occurrence	28	1831
Spinner shark	Occurrence	13	872

true skill statistic ranging from 0.34 to 0.54. The User's and Producer's accuracies showed that absence was consistently predicted more accurately than presence (Table 4).

Across all species, 45 predictor variables were retained in models, with oceanographic predictors being most frequent, followed by prey abundance, substrate, geography, and area of nearby estuarine environments (Fig. 1). Of the 22 oceanographic predictors, the most common predictors were MLD (6), bottom temperature (5), and salinity (5). Of the prey predictor variables, menhaden abundance was not selected as a predictor, but croaker, squid, brown shrimp, and mantis shrimp abundances were selected. Areas of nearby wetlands and estuaries were only tested with sharks, and each shark species was associated with one of these variables. Snapper species were associated with substrate predictors. Three of these variables were related to artificial or natural reefs; sediment grain size, BPI, and distance to shoal were each selected one time. When selected, variable importance varied considerably among variable types, with oceanographic predictors having a high importance value of 18.1 ± 2.5 (mean ± SE) followed by geography (15.8 ± 3.0), prey (12.9 ± 2.2), estuarine habitats (12.8 ± 2.4), and substrate (12 ± 2.7) (Fig. 1).

Table 3. Boosted regression tree specifications, cross-validation, and validation results of species distribution models depicting catch per unit effort (CPUE) or occurrence of select fish species in the northern Gulf of Mexico. TC: tree complexity; AUC: area under the curve statistic for occurrence models; DE: percent deviance explained for CPUE models; R_s: Spearman correlation; NA: not applicable

Species	TC	Number of trees	Cross-validation	Validation	Validation R_s
Red snapper (age 0)	5	1400	DE = 50%	DE = 41%	0.59
Red snapper (age 1)	2	1550	AUC = 0.83	AUC = 0.80	NA
Lane snapper (age 0)	3	1950	AUC = 0.84	AUC = 0.83	NA
Lane snapper (age 1)	2	2550	AUC = 0.91	AUC = 0.89	NA
Atlantic sharpnose shark	5	1900	DE = 45%	DE = 43%	0.60
Blacktip shark	1	1250	AUC = 0.84	AUC = 0.80	NA
Spinner shark	2	1400	AUC = 0.90	AUC = 0.87	NA

Table 4. Error matrices from the validation of fish species distribution models as calculated at the optimal threshold to distinguish presence/absence via the maximum Kappa statistic

Species	Observed absence	Observed presence	User's accuracy (%)
Red snapper (age 1)			
Predicted absence	1323	174	88
Predicted presence	172	207	55
Producer's accuracy	88%	54%	
Overall accuracy = 82%, true skill statistic = 0.43			
Lane snapper (age 0)			
Predicted absence	1185	200	86
Predicted presence	201	290	59
Producer's accuracy	85%	59%	
Overall accuracy = 79%, true skill statistic = 0.45			
Lane snapper (age 1)			
Predicted absence	1379	154	90
Predicted presence	104	238	70
Producer's accuracy	93%	61%	
Overall accuracy = 86%, true skill statistic = 0.54			
Blacktip shark			
Predicted absence	323	61	84
Predicted presence	34	67	66
Producer's accuracy	90%	52%	
Overall accuracy = 80%, true skill statistic = 0.43			
Spinner shark			
Predicted absence	333	76	81
Predicted presence	24	52	68
Producer's accuracy	93%	41%	
Overall accuracy = 79%, true skill statistic = 0.34			

3.2. Snappers

As expected, age-0 red and lane snapper were more abundant in the autumn as individuals grew large enough to be captured by trawl sampling. Each species showed ontogenetic shifts between age 0 and age 1 (Fig. 2). Age-0 red snapper CPUE was most influenced by a positive association with deeper MLD in the summer and spring (Fig. 3). An interaction showed the MLD in summer primarily associated with red snapper captured during the subsequent autumn season (*H*-statistic = 0.23). Additionally, they were positively associated with abundance of brown shrimp, mantis shrimp, and squid. In regard to substrate, age-0 red snapper had an interaction between distance to shoal and BPI (*H*-statistic = 0.55) (Fig. 3; Fig. S1) that showed particularly high CPUE in waters within a close proximity to a shoal and where the BPI showed posi-

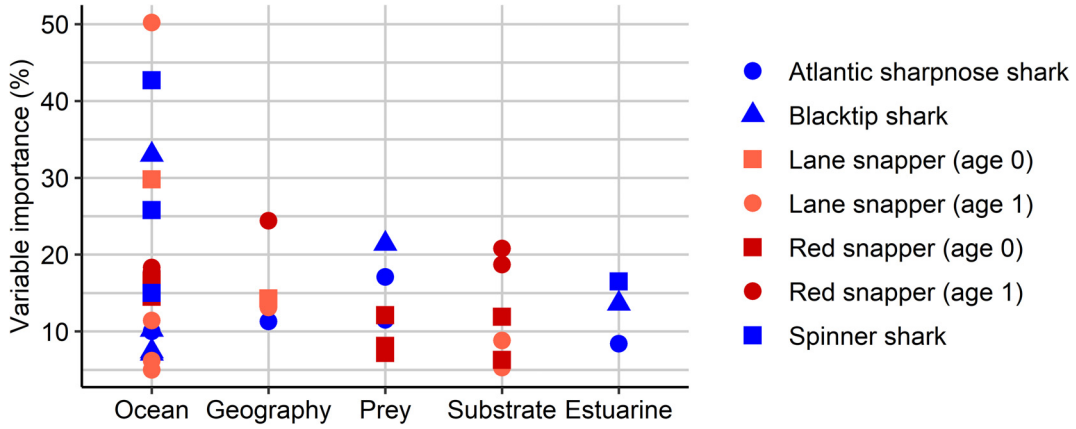

Fig. 1. Frequency and variable importance of predictor variable categories included in species distribution models of shark and snapper species in the Gulf of Mexico, USA. Carcharhinidae include Atlantic sharpnose, blacktip, and spinner sharks. Lutjanidae include age-0 and age-1 lane snapper as well as age-0 and age-1 red snapper

tive topography in the majority of the area. The model of age-1 red snapper was dominated by predictor variable interactions. Age-1 red snapper were farther from shore when within 25 km of artificial structures (*H*-statistic = 0.27) and in waters with a deeper MLD in spring (*H*-statistic = 0.25) (Fig. 4). Because of the high density of artificial structures in the central and western nGoM, this interaction shows that age-1 red snapper move farther offshore in those regions. In contrast, the eastern nGoM has relatively few artificial structures, and the statistical interaction suggests that age-1 red snapper are not as likely to be distributed farther from shore in this region. Similarly, the spring MLD was shallower near Florida, further suggesting that the species does not move farther offshore in the northeastern GoM. Age-1 red snapper had a higher probability of presence within approximately 75 km of natural reefs and at greater depths up to a maximum 50 m depth in the study area.

Age-0 lane snapper were associated with higher spring bottom temperature (>21°C) in combination with higher salinities, particularly salinities of ≥30 psu (*H*-statistic = 0.51). They had a higher probability of presence with higher autumn bottom temperatures (≥27°C), especially where MLD in summer was shallow (*H*-statistic = 0.16) (Fig. 5). Age-0 lane snapper were more prevalent farther from shore.

Age-1 lane snapper had a greater probability of presence in high-salinity waters (≥34 psu), at a greater distance from shore, and with higher autumn temperatures (Fig. 6). They were more likely to occur near artificial structures and in waters <40 m in depth. They were detected less frequently with mud and silt sediment grain sizes (particularly <0.03 mm grain size) and where grain sizes became larger than granule gravel (see Wentworth 1922).

3.3. Sharks

The predicted distribution of the 3 shark species showed they were most common in the western part of the study area (Fig. 7) and likely resulted from their associations with lower salinities and waters with a high area of nearby wetlands and estuaries. Blacktip sharks were positively related to chlorophyll and area of nearby wetlands; they had the highest probability of occurrence in waters with a salinity of 27–34 psu and with higher spring temperatures (≥23.5°C) (Fig. 8). Blacktip sharks were positively related to croaker abundance, but did not show a relationship with menhaden, which are considered by many to be the primary prey of the species. Blacktip sharks were more common where MLD in summer was relatively deep, and they were more likely to be caught between 00:00 and 03:00 h. Interactions were minimal (*H*-statistic <15). Spinner sharks had the highest probability of occurrence with higher chlorophyll concentrations and salinities of ≤30 psu (Fig. 9). Spinner sharks showed an interaction between hypoxia and area of nearby estuaries (*H*-statistic = 0.17), which indicated that occurrence was most likely associated with areas of increased estuarine area coupled with a moderately high probability of hypoxia (Fig. 9).

Atlantic sharpnose shark CPUE was predicted by 8 variables without a particularly dominant variable (Fig. 10). There was a positive association of Atlantic sharpnose shark CPUE with salinities of <30 psu, and

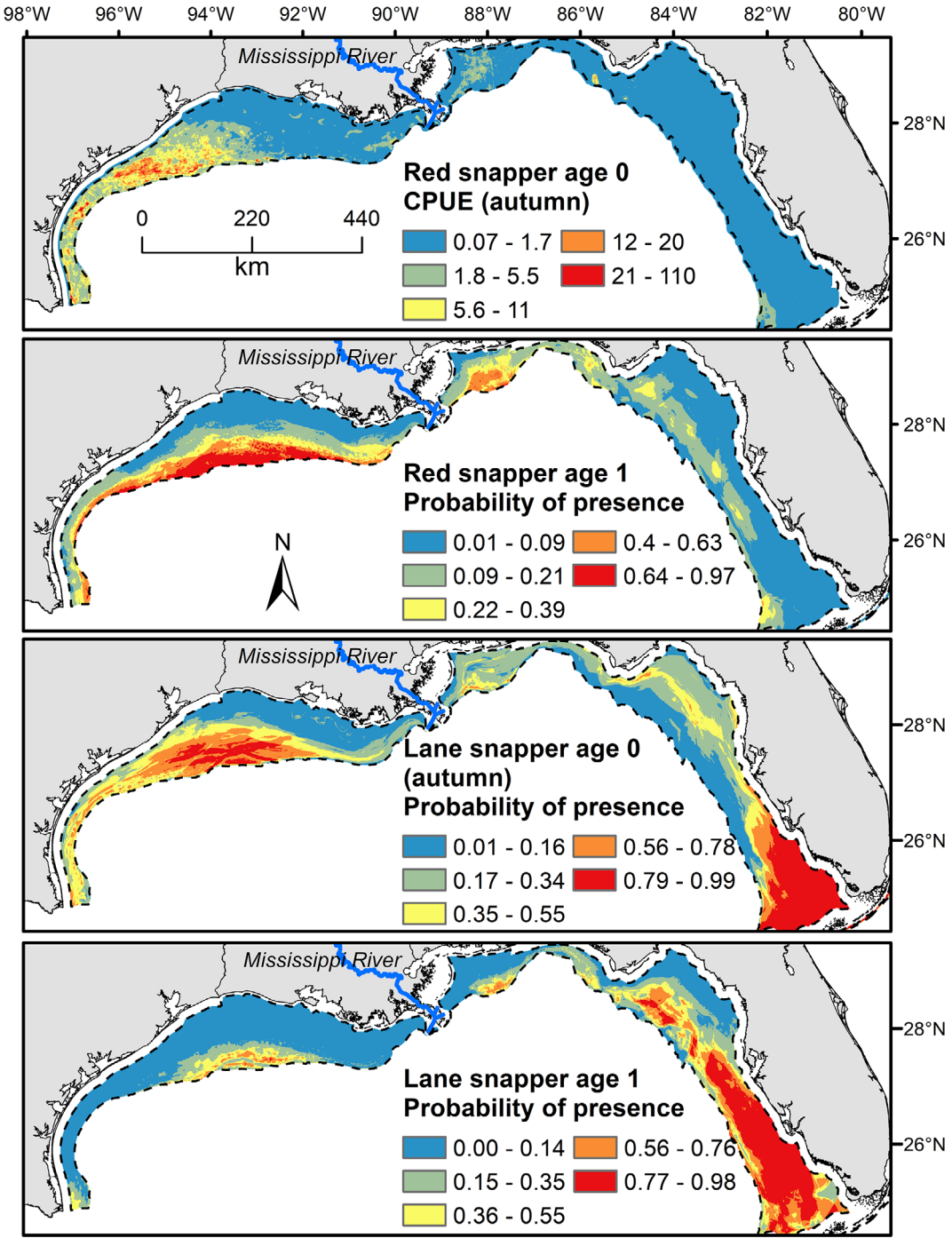

Fig. 2. Predicted distributions of juvenile red snapper and lane snapper by age group. Age-1 depictions include summer and autumn data combined. The study area is indicated by the dashed line, and catch per unit effort (CPUE) represents the predicted number of fish per km of trawl survey

an interaction showed that the effect of salinity was primarily in the spring (*H*-statistic = 0.22). Atlantic sharpnose sharks were positively related to brown shrimp and croaker relative abundance as well as the area of nearby wetlands. Atlantic sharpnose shark CPUE was highest in the spring and at greater depths up to the 50 m maximum in the study area. Another interaction effect showed that CPUE was greater at a farther distance from the shore, particularly where summer MLD was deeper (*H*-statistic = 0.25). An interaction of summer MLD and salinity showed that CPUE was greater where low salinity combined with a deeper summer MLD (*H*-statistic = 0.19).

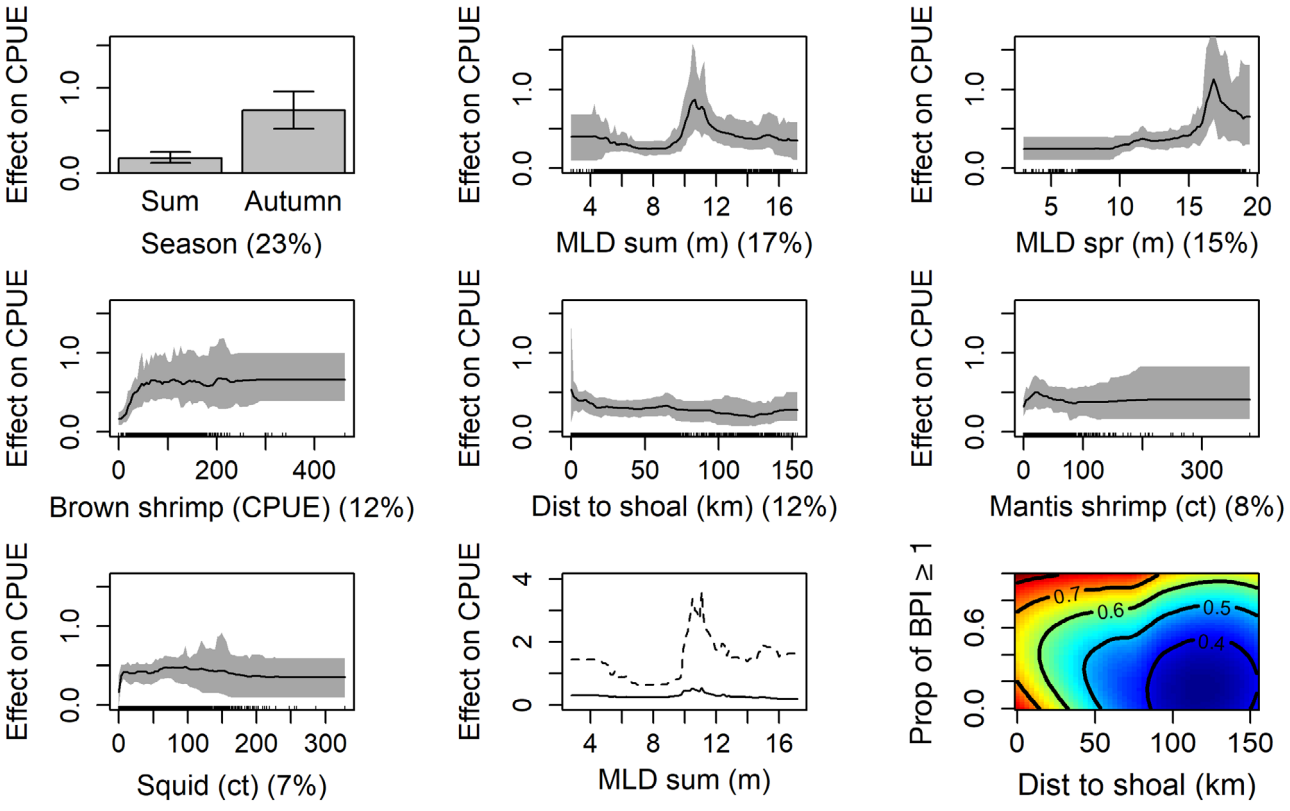

Fig. 3. Partial dependence plots of the age-0 red snapper boosted regression tree model with catch per unit effort (CPUE) as the dependent variable. Gray shadings are 95% prediction intervals determined from bootstrap analysis. Data distribution is represented in the rug plot along the *x*-axis, and variable importance (%) is given on the *x*-axis label. The plot with 2 response curves and a *y*-axis scaled to a maximum of 4 CPUE shows the interaction of mixed layer depth (MLD) in summer with red snapper in autumn (dashed line) and summer (solid line) seasons. Interaction plot of distance to shoal×proportion of area with a bathymetric position index (BPI) ≥1 shows the effect on CPUE as indicated by color and contour lines; sum: summer; spr: spring; Dist to shoal: distance to shoal; ct: count; Prop of BPI ≥ 1: proportion of area with a bathymetric position index ≥1

4. DISCUSSION

Because marine predators face anthropogenic threats such as alterations to coastal habitats, pollution, and climate change, there is an urgent need to identify how predators are expected to respond to changes in these variables (Knip et al. 2010, Spaet et al. 2020). Models integrated multiscale environmental datasets, of which the oceanographic variables were the most important predictors in 6 of the 8 models. As hypothesized, all 3 shark species were positively associated with either area of nearby wetlands or area of nearby estuaries (Figs. 8–10). Prey species distributions were positively associated with snapper and sharks, with total variable importance of prey within models ranging from 21 to 49% (Figs. 3, 8, & 10). The response curves of species relationships with area of nearby estuarine habitats and prey species were similar across species. Additionally, the advantages of machine learning analyses were demonstrated by the identification of important ecological interactions, which would have otherwise gone untested. The novel species–habitat associations quantified here are expected to contribute to defining essential fish habitat for each species.

4.1. Associations with area of nearby wetlands and estuaries

Our findings provide further evidence for the concept of outwelling, as the area of nearby estuarine environments was consistently correlated with the distribution of sharks in the marine environment. In a review of marine megafauna associations with coastal wetlands, Sievers et al. (2019) showed that seagrass, and to a lesser extent mangroves, have been associated with a variety of shark life stages (Driggers et al. 2014). The value of estuarine waters as shark nurseries has been well-recognized (Heupel et al. 2007); however, our study is the first to link the distribution of sharks in the offshore marine

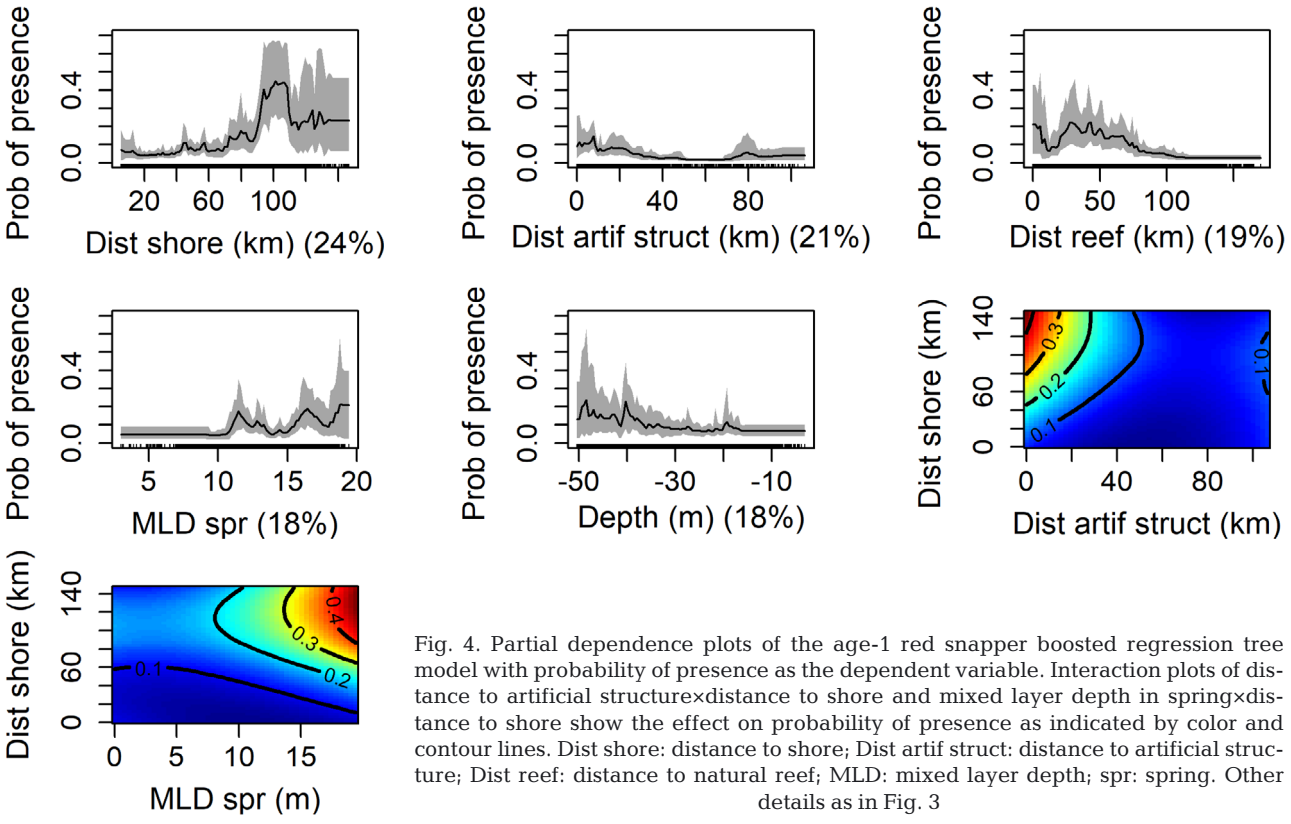

Fig. 4. Partial dependence plots of the age-1 red snapper boosted regression tree model with probability of presence as the dependent variable. Interaction plots of distance to artificial structure×distance to shore and mixed layer depth in spring×distance to shore show the effect on probability of presence as indicated by color and contour lines. Dist shore: distance to shore; Dist artif struct: distance to artificial structure; Dist reef: distance to natural reef; MLD: mixed layer depth; spr: spring. Other details as in Fig. 3

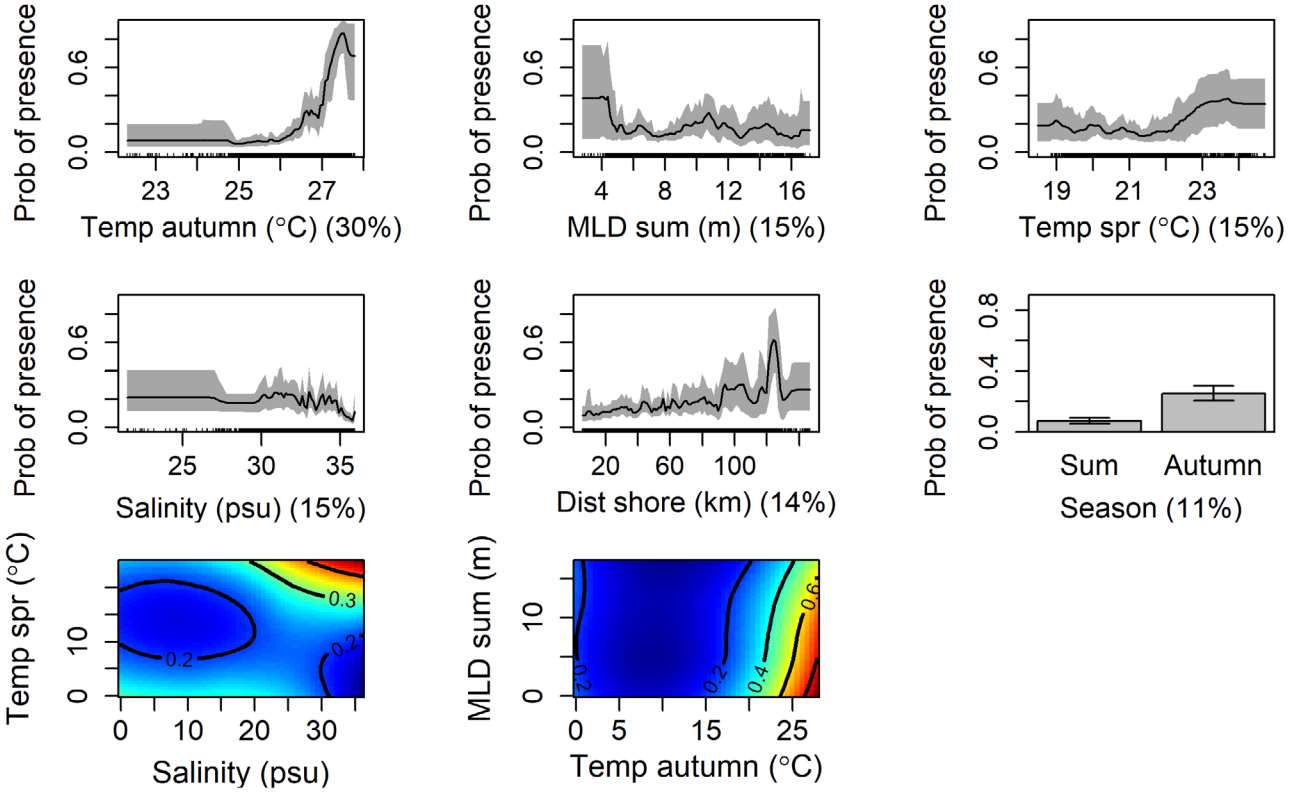

Fig. 5. Partial dependence plots of the age-0 lane snapper boosted regression tree model with probability of presence as the dependent variable. Interaction plots of salinity×temperature in spring and temperature in autumn×mixed layer depth in summer show the effect on probability of presence as indicated by color and contour lines. Temp: temperature; MLD: mixed layer depth; sum: summer; spr: spring; Dist shore: distance to shore. Other details as in Fig. 3

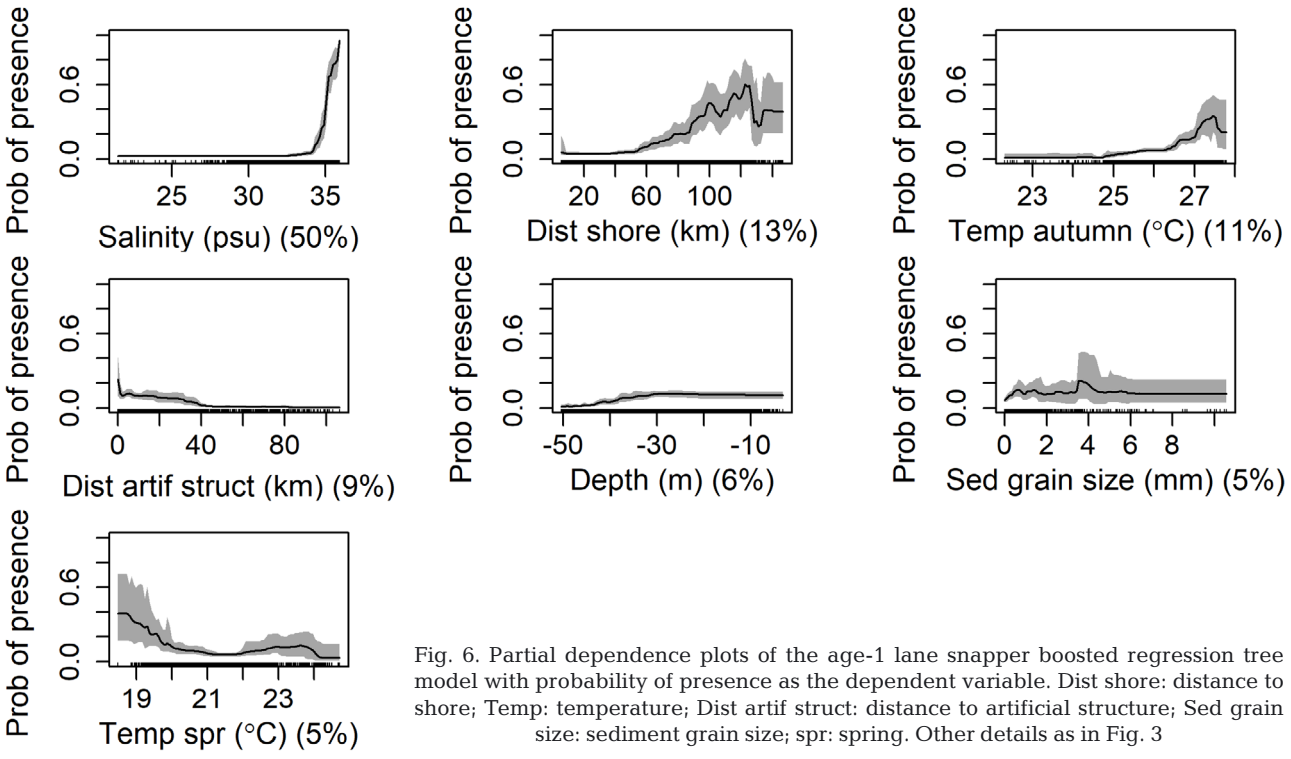

Fig. 6. Partial dependence plots of the age-1 lane snapper boosted regression tree model with probability of presence as the dependent variable. Dist shore: distance to shore; Temp: temperature; Dist artif struct: distance to artificial structure; Sed grain size: sediment grain size; spr: spring. Other details as in Fig. 3

environment with nearby, or adjacent, coastal wetlands and estuaries. Given the widespread geographic distribution of salt marshes in the world (Hoekstra et al. 2010), this association warrants further attention. Variables depicting distance to shore are relatively common in marine SDMs (Melo-Merino et al. 2020), but only a few studies have linked marine fish or shrimp distribution to the proximity of adjacent ecosystems (Pickens et al. 2021c). Such studies have found that the proximity of mangroves (Barbier & Strand 1998), estuaries (Beger & Possingham 2008, Sundblad et al. 2014), and wetlands (Pickens et al. 2021a) have been associated with marine species distributions. Our findings suggest that a more detailed analysis of the marine–land interface is needed to improve our understanding of the spatial scale influenced by estuarine environments and to quantify variables most relevant to species such as area, number of habitat patches, connectivity, river outflow, or indices of productivity. This is in agreement with Pittman et al. (2021), who suggested that we need to shift our perspective to understand patch mosaics in seascapes rather than treating the marine environment as a singular unit. Our study adds to research that has demonstrated the importance of connectivity of marine environments to estuaries, seagrass, wetlands, and freshwater environments (Sheaves 2009, Olds et al. 2012). Our findings of fish associations with prey species also illustrates the importance of estuarine environments.

4.2. Associations with prey

Age-0 red snapper and Atlantic sharpnose sharks were positively associated with the estuarine-dependent brown shrimp. The brown shrimp CPUE model was primarily based on predictors of MLD and nearby wetland area (Pickens et al. 2021a), which further highlights the role of estuarine habitats. Blacktip and Atlantic sharpnose shark distributions were predicted by the abundance of croaker, which utilize both estuarine and marine environments. The inclusion of biotic predictor variables can increase the predictive ability of models (Bennington et al. 2020, Costa et al. 2020), but Pickens et al. (2021c) found that only 3% of marine fish SDMs published since 2007 have considered biotic variables. Across the species examined here, the predator–prey response curves were similar in shape to a type II or III curve of Holling (1959). The Holling response curves show that as prey density increases, predators initially respond positively with increased consumption followed by a plateau where the effect is minimal. Evidence of this response has been found with lower trophic level marine fishes on the US continental shelf (Moustahfid et al. 2010), and our findings sug-

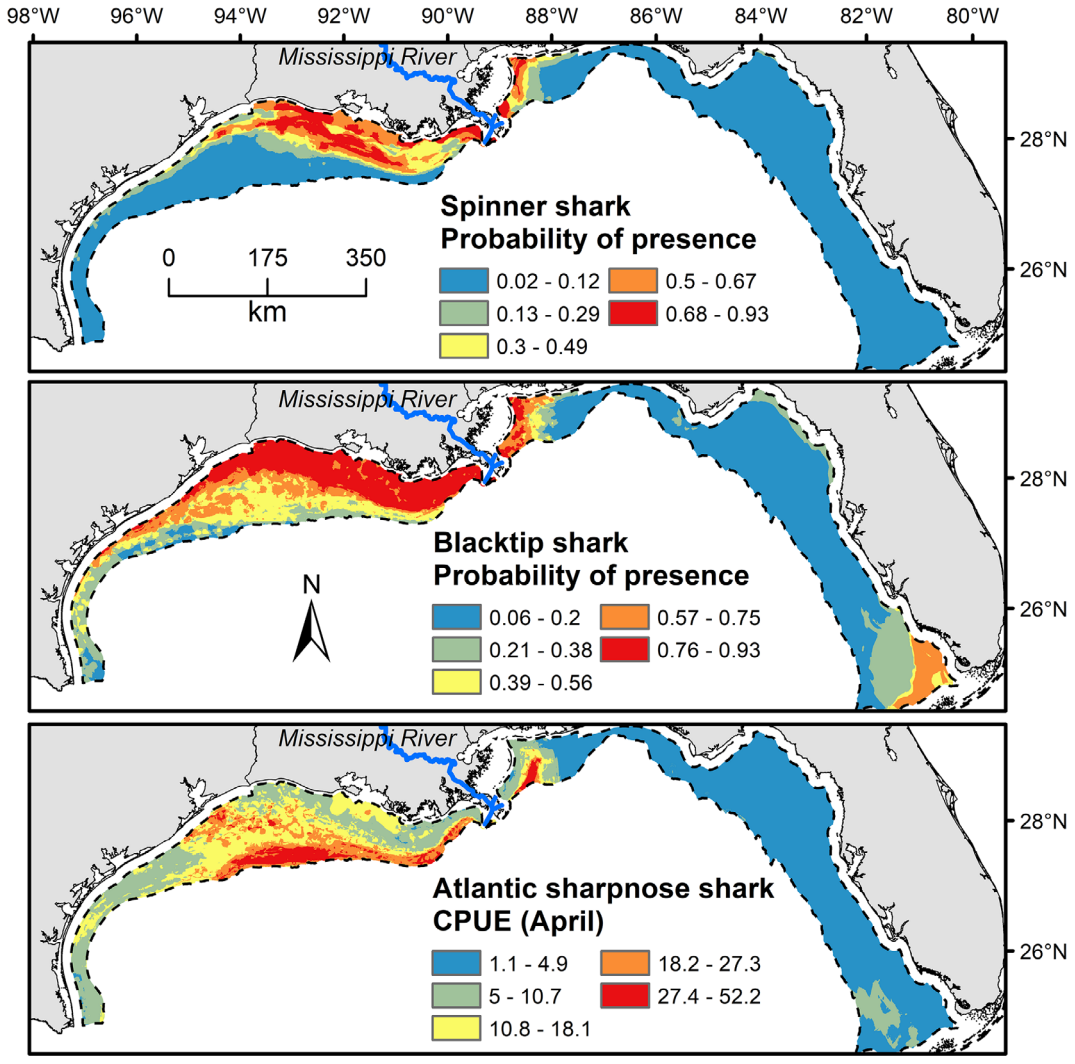

Fig. 7. Predicted distributions of spinner shark, blacktip shark, and Atlantic sharpnose shark. The study area is indicated by the dashed line, and probability of presence represents the probability of capture given a bottom longline survey. Catch per unit effort (CPUE) is measured in individuals per 100 hooks per hour of bottom longline survey

gest a similar response may occur with predator distributions. For sharks in particular, we are aware of only 1 article that has tested a predator–prey relationship in an SDM. Manderson et al. (2011) found that squid abundance explained a minor amount of variance in the distribution of spiny dogfish *Squalus acanthias*. In our study, blacktip sharks were positively correlated with croaker, but we did not find blacktip or spinner sharks to be correlated with what is reported to be their primary prey, menhaden. A possible explanation for this is that bottom trawl surveys are poor at sampling pelagic menhaden. However, both shark species were associated with characteristics that describe menhaden habitat. Gulf menhaden utilize estuary and nearshore waters of moderate salinity, where they prey directly on phytoplankton and zooplankton (Olsen et al. 2014). These prey are likely correlated with chlorophyll *a* measures. Gulf menhaden use estuaries and open water–marsh edges (Rozas et al. 2007, Rozas & Minello 2015); therefore, a shark association with these habitats is expected. Spinner sharks have been found in waters with relatively low dissolved oxygen (Drymon et al. 2013). We found a positive relationship between spinner sharks and hypoxia with a peak probability of occurrence with a 25–40% frequency of hypoxia. These results suggest that spinner sharks may feed on prey that either aggregate at the edge of hypoxic zones (e.g. Craig 2012) or aggregate toward the surface (e.g. Hazen et al. 2009). In lab experiments, Atlantic menhaden *Brevoortia tyrannus* avoided waters with low dissolved oxygen (Wannamaker & Rice 2000), and this is the case in the region evaluated in our study.

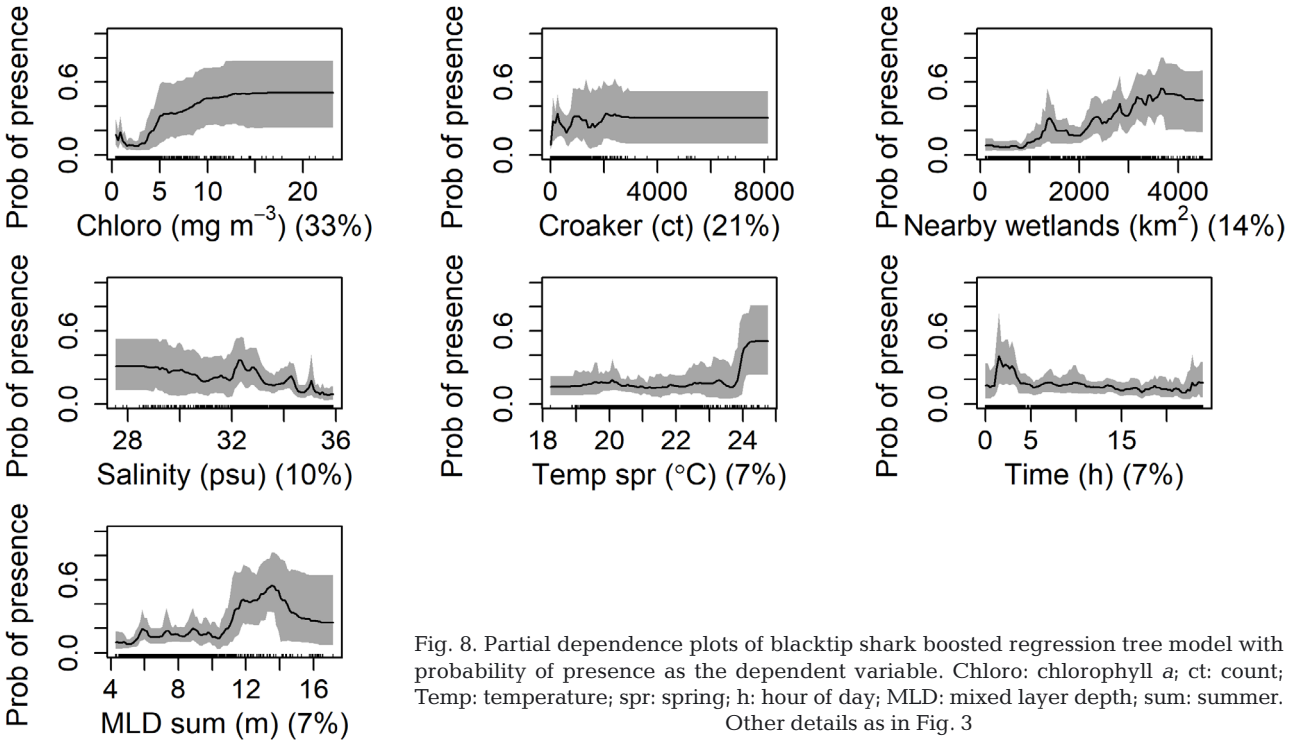

Fig. 8. Partial dependence plots of blacktip shark boosted regression tree model with probability of presence as the dependent variable. Chloro: chlorophyll *a*; ct: count; Temp: temperature; spr: spring; h: hour of day; MLD: mixed layer depth; sum: summer. Other details as in Fig. 3

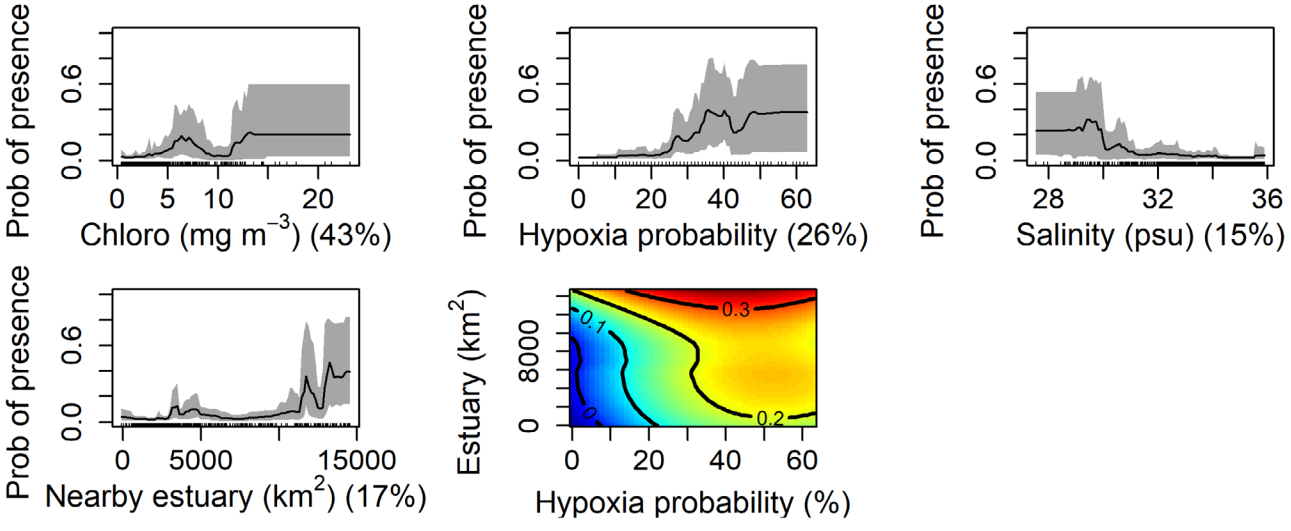

Fig. 9. Partial dependence plots of spinner shark boosted regression tree model with probability of presence as the dependent variable. Interaction plot of hypoxia probability×area of nearby estuaries shows the effect on probability of presence as indicated by color and contour lines. Chloro: chlorophyll *a*; Estuary = area of nearby estuaries. Other details as in Fig. 3

4.3. Associations with oceanography and substrate

Salinity and chlorophyll were expected to be important predictors of species distributions in the study area, but the frequency and importance of the MLD predictor was unexpected. MLD was a predictor of distributions of age-0 and age-1 red snapper, age-0 lane snapper, blacktip sharks, and Atlantic sharpnose sharks. In the nGoM, MLD appears to be influenced by the Loop Current, eddies, and wind stress. The Loop Current circulates in the central GoM, and produces large spin-off eddies that often take a westward path originating near the Mississippi Delta (Johnson et al. 2017). To a lesser extent, wind influences water vertical structure and contributes to the vorticity of eddies (Ohlmann et al. 2001). The overall result is an exchange of shelf waters and deeper waters (Ohlmann et al. 2001,

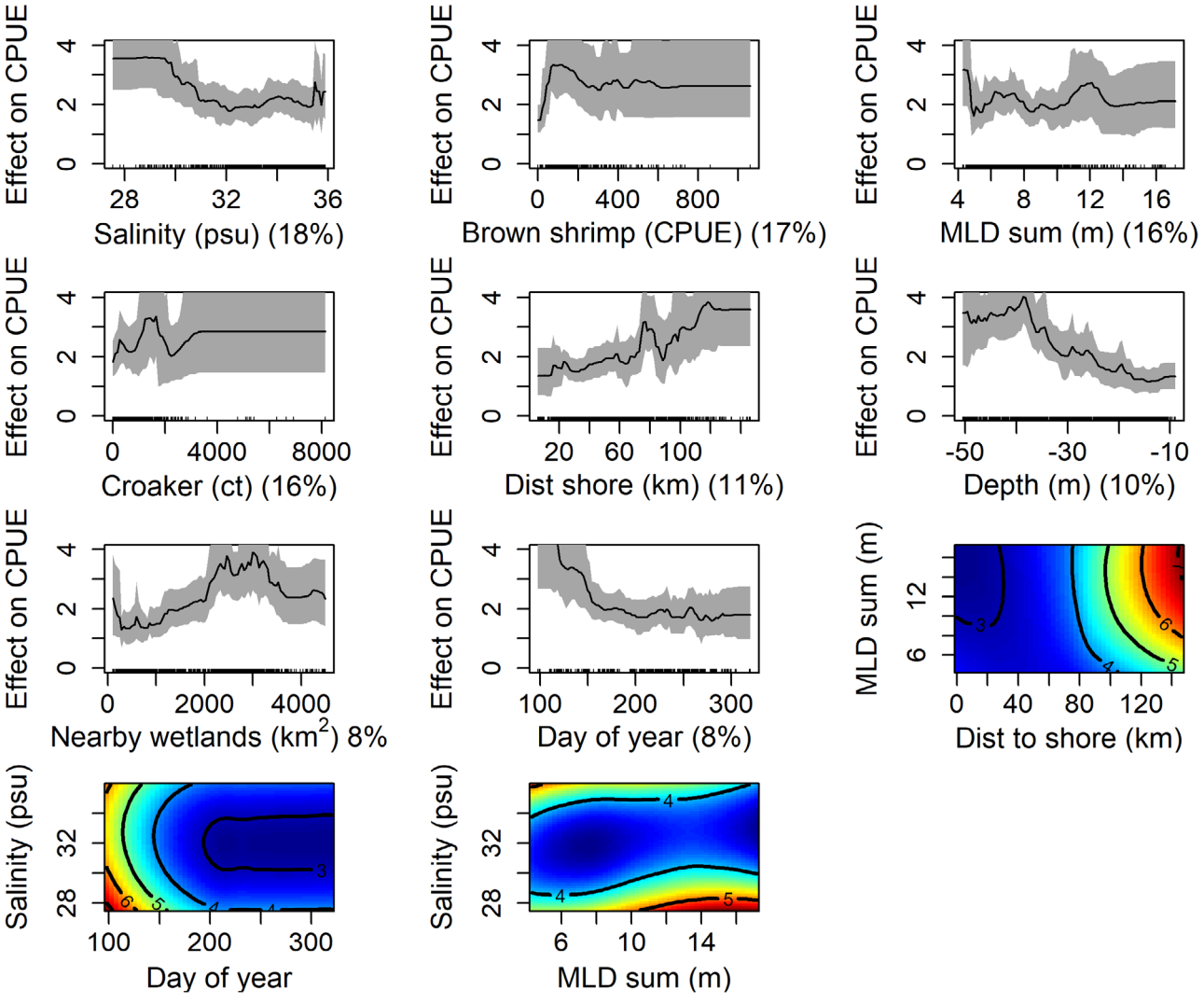

Fig. 10. Partial dependence plots of the Atlantic sharpnose shark boosted regression tree model with catch per unit effort (CPUE) as the dependent variable. Interaction plots of distance to shore×MLD summer, day of year×salinity, and MLD summer×salinity show the effect on CPUE as indicated by color and contour lines. MLD: mixed layer depth; sum: summer; ct: count; Dist shore: distance to shore. Other details as in Fig. 3

Johnson et al. 2017), which contributes to biological productivity via upwelling or downwelling (Spies et al. 2016). The MLD predictor may complement the productivity measure of chlorophyll because satellite-derived chlorophyll concentrations are restricted to the water surface. The frequency and strength of associations with MLD suggest that it should be considered in future research. Hypoxia was only a predictor of spinner shark distribution, although waters with a high frequency of hypoxia were predicted to have a low CPUE, or probability of presence, of Atlantic sharpnose sharks and all age classes of red and lane snapper. Switzer et al. (2015) found that the relative abundance of juvenile red snapper in shallow waters was reduced during years with severe hypoxia, and they appear to have moved to deeper, cooler waters during those years. Similarly, brown shrimp shift their distribution in terms of depth and temperature in response to hypoxic conditions (Craig & Crowder 2005). In our study, the correlation of brown shrimp prey with the demersal age-0 red snapper and Atlantic sharpnose sharks may have indirectly represented low prey abundances near hypoxic waters. From a broad perspective, these associations provide evidence that the shifting of brown shrimp distributions may affect fish at higher trophic levels.

Substrate predictors were only retained in models of juvenile red and lane snapper, which is in agreement with their ecology. We found that age-0 red snapper had an interaction showing they were more abundant in close proximity to sand shoals, particu-

larly when the BPI showed high topographic relief, while age-1 lane snapper were associated with sand sediment grain sizes. These findings demonstrate that models with a broad spatial extent can quantify fine-scale habitat associations, although broad influences, such as oceanographic conditions, may limit the importance of substrate characteristics. For example, the distribution of age-0 red snapper was highly skewed towards the northwestern GoM, where MLD was deeper and brown shrimp prey were most abundant. The partial dependence plot of the age-1 lane snapper model (Fig. 6) showed salinity to be the most important variable and it had narrow confidence intervals, which suggests the species did not occupy waters <34 psu. Meanwhile, sediment grain size was the sixth most important variable.

A distinct ontogenetic shift occurred from age-0 to age-1 red and lane snapper (Fig. 2), which appears driven by fish movement farther offshore and towards structured habitats such as natural reefs and artificial structures. BRTs automatically test interaction terms because of the model structure, and we found that age-1 red snapper moved farther offshore where they were in close proximity to an artificial structure or where spring MLD was deeper (Fig. 4). The vast majority of waters in the northwestern GoM are within 40 km of an artificial structure because of oil and gas infrastructure, but relatively few artificial structures exist in the northeastern GoM. Furthermore, the northeastern GoM also corresponds with abundant natural reef substrates, and juvenile red snapper may not need to go offshore to find appropriate substrates to meet adult life history requirements. Dance & Rooker (2019) found a spatially similar ontogenetic shift of juvenile red snapper, but major variable contributions were derived from latitude, longitude, and depth. In our study, oceanographic variables such as MLD characterized the dominant patterns, but the age-0 model included locally recognized habitat requirements of prey and topographic complexity that lead to a more mechanistic understanding of snapper distribution. Our findings of age-1 red and lane snapper with natural reefs and artificial structures are consistent with their ecology of moving to more complex substrates with age.

4.4. Conclusions

We found that multiscale predictors characterizing the ocean, prey species, substrate, and area of nearby wetlands and estuaries all play roles in determining species distributions in the marine environment. Machine learning provided an effective means to incorporate numerous predictors and to test interactions. Our study builds upon fish species distribution modeling that has focused on depth, temperature, and geographic gradients as predictors. The selection of variables is key to SDM development (Elith & Leathwick 2009), and predictors are best derived from ecological knowledge and hypothesized species–environment relationships (Mac Nally 2000, Araujo & Guisan 2006). Here, we tested novel variables to improve upon current knowledge of fish habitat requirements and to inform management of fish and the ocean environment. In agreement with Sievers et al. (2019), we suggest that the effect of coastal wetlands, and their productivity, needs further consideration in shark studies. This association has major implications for sharks because of the threats of sea-level rise, wetland loss, and pollution of estuaries. The importance and scale of fish–substrate associations has implications with ocean uses, such as sand mining, oil and gas infrastructure, and renewable energy development. We acknowledge that our analyses were based on fisheries-independent survey gears and methods that typically span 3 km in length. Habitat selection at finer spatial scales were not quantified. Yet, our models showed a high predictive ability and were able to quantify hypothesized relationships.

Acknowledgements. NOAA and the Bureau of Ocean Energy Management (BOEM) funded this work through interagency agreement #M17PG00028. B.A.P. was supported by CSS-Inc. under NOAA/NCCOS contract #GS-00F-217CA. The University of North Carolina Wilmington Center for Marine Science provided logistical support. Dr. Dan Obenour and Rohith Matli of North Carolina State University provided data on probability of hypoxia occurrence. We thank the BOEM staff as well as Arliss Winship and Matthew Poti (CSS-Inc. and affiliates of the NOAA Biogeography Branch) for their review of an earlier draft of this manuscript.

LITERATURE CITED

Allouche O, Tsoar A, Kadmon R (2006) Assessing the accuracy of species distribution models: prevalence, kappa and the true skill statistic (TSS). J Appl Ecol 43:1223–1232

Araujo MB, Guisan A (2006) Five (or so) challenges for species distribution modelling. J Biogeogr 33:1677–1688

Austin M (2002) Spatial prediction of species distribution: an interface between ecological theory and statistical modelling. Ecol Model 157:101–118

Barbier EB, Strand I (1998) Valuing mangrove–fishery linkages — a case study of Campeche, Mexico. Environ Resour Econ 12:151–166

Barry K, Condrey R, Driggers W, Jones C (2008) Feeding ecology and growth of neonate and juvenile blacktip sharks *Carcharhinus limbatus* in the Timbalier–Terrebone Bay complex, LA, USA. J Fish Biol 73:650–662

Beger M, Possingham HP (2008) Environmental factors that influence the distribution of coral reef fishes: modeling occurrence data for broad-scale conservation and management. Mar Ecol Prog Ser 361:1–13

Bennington S, Rayment W, Dawson S (2020) Putting prey into the picture: improvements to species distribution models for bottlenose dolphins in Doubtful Sound, New Zealand. Mar Ecol Prog Ser 653:191–204

Bethea DM, Buckel JA, Carlson JK (2004) Foraging ecology of the early life stages of four sympatric shark species. Mar Ecol Prog Ser 268:245–264

Bradley E, Bryan C (1975) Life history and fishery of the red snapper (*Lutjanus campechanus*) in the northwestern Gulf of Mexico 1970–1974. In: Proc 27th Gulf and Caribbean Fisheries Institute, University of Miami, Miami, FL, p 77–106

Bureau of Safety and Environmental Enforcement Gulf of Mexico OCS Region (2014) Outer continental shelf oil and natural gas platforms – Gulf of Mexico region NAD 27. www.data.boem.gov/Mapping/Files/platform.zip (accessed 15 Mar 2018)

Chassignet EP, Hurlburt HE, Metzger EJ, Smedstad OM and others (2009) US GODAE: global ocean prediction with the HYbrid Coordinate Ocean Model (HYCOM). Oceanography 22:64–75

Chong VC (2007) Mangroves–fisheries linkages — the Malaysian perspective. Bull Mar Sci 80:755–772

Cortés E (1999) Standardized diet compositions and trophic levels of sharks. ICES J Mar Sci 56:707–717

Costa PL, Bugoni L, Kinas PG, Madureira LASP (2020) Seabirds, environmental features and the Argentine anchovy *Engraulis anchoita* in the southwestern Atlantic Ocean. Mar Ecol Prog Ser 651:199–213

Craig JK (2012) Aggregation on the edge: effects of hypoxia avoidance on the spatial distribution of brown shrimp and demersal fishes in the Northern Gulf of Mexico. Mar Ecol Prog Ser 445:75–95

Craig JK, Crowder LB (2005) Hypoxia-induced habitat shifts and energetic consequences in Atlantic croaker and brown shrimp on the Gulf of Mexico shelf. Mar Ecol Prog Ser 294:79–94

Dance MA, Rooker JR (2019) Cross-shelf habitat shifts by red snapper (*Lutjanus campechanus*) in the Gulf of Mexico. PLOS ONE 14:e0213506

De'ath G (2007) Boosted trees for ecological modeling and prediction. Ecology 88:243–251

De'ath G, Fabricius KE (2000) Classification and regression trees: a powerful yet simple technique for ecological data analysis. Ecology 81:3178–3192

Deegan LA (1993) Nutrient and energy transport between estuaries and coastal marine ecosystems by fish migration. Can J Fish Aquat Sci 50:74–79

Deegan LA, Hughes JE, Rountree RA (2002) Salt marsh ecosystem support of marine transient species. In: Weinstein MP, Kreeger DA (eds) Concepts and controversies in tidal marsh ecology. Springer, Dordrecht, p 333–365

Delorenzo DM, Bethea DM, Carlson JK (2015) An assessment of the diet and trophic level of Atlantic sharpnose shark *Rhizoprionodon terraenovae.* J Fish Biol 86: 385–391

Drabble R (2012) Monitoring of East Channel dredge areas benthic fish population and its implications. Mar Pollut Bull 64:363–372

Driggers WB III, Campbell MD, Hoffmayer ER, Ingram GW Jr (2012) Feeding chronology of six species of carcharhinid sharks in the western North Atlantic Ocean as inferred from longline capture data. Mar Ecol Prog Ser 465:185–192

Driggers WB III, Frazier BS, Adams DH, Ulrich GF, Jones CM, Hoffmayer ER, Campbell MD (2014) Site fidelity of migratory bonnethead sharks *Sphyrna tiburo* (L. 1758) to specific estuaries in South Carolina, USA. J Exp Mar Biol Ecol 459:61–69

Drymon JM, Powers SP, Carmichael RH (2012) Trophic plasticity in the Atlantic sharpnose shark (*Rhizoprionodon terraenovae*) from the north central Gulf of Mexico. Environ Biol Fishes 95:21–35

Drymon JM, Carassou L, Powers SP, Grace M, Dindo J, Dzwonkowski B (2013) Multiscale analysis of factors that affect the distribution of sharks throughout the northern Gulf of Mexico. Fish Bull 111:370–380

Elith J, Leathwick JR (2009) Species distribution models: ecological explanation and prediction across space and time. Annu Rev Ecol Evol Syst 40:677–697

Elith J, Leathwick JR, Hastie T (2008) A working guide to boosted regression trees. J Anim Ecol 77:802–813

Fourcade Y, Besnard AG, Secondi J (2018) Paintings predict the distribution of species, or the challenge of selecting environmental predictors and evaluation statistics. Glob Ecol Biogeogr 27:245–256

Franks JS, VanderKooy KE (2000) Feeding habits of juvenile lane snapper *Lutjanus synagris* from Mississippi coastal waters, with comments on the diet of gray snapper *Lutjanus griseus.* Gulf Caribb Res 12:11–17

Friedman JH (2001) Greedy function approximation: a gradient boosting machine. Ann Stat 29:1189–1232

Friedman JH, Meulman JJ (2003) Multiple additive regression trees with application in epidemiology. Stat Med 22: 1365–1381

Friedman JH, Popescu BE (2008) Predictive learning via rule ensembles. Ann Appl Stat 2:916–954

Geers T, Pikitch E, Frisk M (2016) An original model of the northern Gulf of Mexico using Ecopath with Ecosim and its implications for the effects of fishing on ecosystem structure and maturity. Deep Sea Res II 129:319–331

Guisan A, Zimmermann NE (2000) Predictive habitat distribution models in ecology. Ecol Modell 135:147–186

Guisan A, Tingley R, Baumgartner JB, Naujokaitis-Lewis I and others (2013) Predicting species distributions for conservation decisions. Ecol Lett 16:1424–1435

Harrington T, Plumlee J, Drymon JM, Wells D (2016) Diets of Atlantic sharpnose shark (*Rhizoprionodon terraenovae*) and bonnethead (*Sphyrna tiburo*) in the northern Gulf of Mexico. Gulf Caribb Res 27:42–51

Hazen EL, Craig JK, Good CP, Crowder LB (2009) Vertical distribution of fish biomass in hypoxic waters on the Gulf of Mexico shelf. Mar Ecol Prog Ser 375:195–207

Heupel MR, Carlson JK, Simpfendorfer CA (2007) Shark nursery areas: concepts, definition, characterization and assumptions. Mar Ecol Prog Ser 337:287–297

Hobday AJ, Hartog JR (2014) Derived ocean features for dynamic ocean management. Oceanography 27:134–145

Hoekstra JM, Molnar JL, Jennings M, Revenga C and others (2010) The atlas of global conservation: changes, challenges, and opportunities to make a difference. University of California Press, Berkeley, CA

Holling CS (1959) The components of predation as revealed by a study of small mammal predation of the European pine sawfly. Can Entomol 91:293–320

Hwang SW, Lee HG, Choi KH, Kim CK, Lee TW (2013) Im-

pact of sand extraction on fish assemblages in Gyeonggi Bay, Korea. J Coast Res 30:1251–1259

Johnson DR, Perry H, Sanchez-Rubio G, Grace MA (2017) Loop current spin-off eddies, slope currents and dispersal of reef fish larvae from the flower gardens National Marine Sanctuary and the Florida middle grounds. Gulf Caribb Res 28:29–39

JPL MUR MEaSUREs Project (2015) GHRSST level 4 MUR Global Foundation sea surface temperature analysis Ver. 4.1. PO.DAAC. http://dx.doi.org/10.5067/GHGMR-4FJ04 (accessed 2 Apr 2019)

Kearney M, Porter W (2009) Mechanistic niche modelling: combining physiological and spatial data to predict species' ranges. Ecol Lett 12:334–350

Kim TG, Grigalunas TA, Han KN (2008) The economic costs to fisheries because of marine sand mining in Ongjin Korea: concepts, methods, and illustrative results. Ecol Econ 65:498–507

Knip DM, Heupel MR, Simpfendorfer CA (2010) Sharks in nearshore environments: models, importance, and consequences. Mar Ecol Prog Ser 402:1–11

Mac Nally R (2000) Regression and model-building in conservation biology, biogeography and ecology: the distinction between –and reconciliation of– 'predictive' and 'explanatory' models. Biodivers Conserv 9:655–671

Manderson J, Palamara L, Kohut J, Oliver MJ (2011) Ocean observatory data are useful for regional habitat modeling of species with different vertical habitat preferences. Mar Ecol Prog Ser 438:1–17

Mannocci L, Boustany AM, Roberts JJ, Palacios DM and others (2017) Temporal resolutions in species distribution models of highly mobile marine animals: recommendations for ecologists and managers. Divers Distrib 23: 1098–1109

Marin-Enriquez E, Seoane J, Muhlia-Melo A (2018) Environmental modeling of occurrence of dolphinfish (*Coryphaena* spp.) in the Pacific Ocean off Mexico reveals seasonality in abundance, hot spots and migration patterns. Fish Oceanogr 27:28–40

Martin TSH, Olds AD, Pitt KA, Johnston AB, Butler IR, Maxwell PS, Connolly RM (2015) Effective protection of fish on inshore coral reefs depends on the scale of mangrove–reef connectivity. Mar Ecol Prog Ser 527:157–165

Matli VRR, Fang SQ, Guinness J, Rabalais NN, Craig JK, Obenour DR (2018) Space–time geostatistical assessment of hypoxia in the northern Gulf of Mexico. Environ Sci Technol 52:12484–12493

Melo-Merino SM, Reyes-Bonilla H, Lira-Noriega A (2020) Ecological niche models and species distribution models in marine environments: a literature review and spatial analysis of evidence. Ecol Model 415:108837

Montero JT, Chesney TA, Bauer JR, Froeschke JT, Graham J (2016) Brown shrimp (*Farfantepenaeus aztecus*) density distribution in the northern Gulf of Mexico: an approach using boosted regression trees. Fish Oceanogr 25:337–348

Moore C, Drazen JC, Radford BT, Kelley C, Newman SJ (2016) Improving essential fish habitat designation to support sustainable ecosystem-based fisheries management. Mar Policy 69:32–41

Moustahfid H, Tyrrell M, Link J, Nye J, Smith B, Gamble R (2010) Functional feeding responses of piscivorous fishes from the northeast US continental shelf. Oecologia 163: 1059–1067

NOAA National Centers for Environmental Information (2010) US coastal relief model. www.ngdc.noaa.gov/mgg/coastal/crm.html (accessed 2 Mar 2018)

NOAA National Centers for Environmental Information (2019) Gulf of Mexico hypoxia watch. www.ncei.noaa.gov/maps/hypoxia/ (accessed 7 Jan 2021)

NOAA National Marine Fisheries Service (2019) Red drum essential fish habitat (EFH) map and GIS data. https://www.fisheries.noaa.gov/resource/map/red-drum-essential-fish-habitat-efh-map-gis-data (accessed 8 Apr 2019)

Odum EP (1980) The status of three ecosystem-level hypotheses regarding salt marsh estuaries: tidal subsidy, outwelling, and detritus-based food chains. In: Kennedy VS (ed) Estuarine perspectives. Elsevier, New York, NY, p 485–495

Office for Coastal Management (2017) Artificial reefs. https://marinecadastre.gov/data/ (accessed 15 Mar 2018)

Office for Coastal Management (2020) Outer Continental Shelf Lands Act. https://inport.nmfs.noaa.gov/inport/item/48913 (accessed 6 Aug 2018)

Ohlmann JC, Niiler PP, Fox CA, Leben RR (2001) Eddy energy and shelf interactions in the Gulf of Mexico. J Geophys Res C Oceans 106:2605–2620

Olds AD, Connolly RM, Pitt KA, Maxwell PS (2012) Primacy of seascape connectivity effects in structuring coral reef fish assemblages. Mar Ecol Prog Ser 462:191–203

Olsen Z, Fulford R, Dillon K, Graham W (2014) Trophic role of gulf menhaden *Brevoortia patronus* examined with carbon and nitrogen stable isotope analysis. Mar Ecol Prog Ser 497:215–227

Pennino MG, Conesa D, Lopez-Quilez A, Munoz F, Fernandez A, Bellido JM (2016) Fishery-dependent and -independent data lead to consistent estimations of essential habitats. ICES J Mar Sci 73:2302–2310

Pickens BA, Carroll R, Taylor JC (2021a) Predicting the distribution of penaeid shrimp reveals linkages between estuarine and marine habitats. Estuar Coasts 44:2265–2278

Pickens BA, Taylor JC, Finkbeiner M, Hansen D, Turner L (2021b) Modeling sand shoals on the US Atlantic Shelf: moving beyond a site-by-site approach. J Coast Res 37: 227–237

Pickens BA, Carroll R, Schirripa MJ, Forrestal F, Friedland KD, Taylor JC (2021c) A systematic review of spatial habitat associations and modeling of marine fish distribution: a guide to predictors, methods, and knowledge gaps. PLOS ONE 16:e0251818

Pittman SJ, Kneib RT, Simenstad CA (2011) Practicing coastal seascape ecology. Mar Ecol Prog Ser 427:187–190

Pittman SJ, Yates KL, Bouchet PJ, Alvarez-Berastegui D and others (2021) Seascape ecology: identifying research priorities for an emerging ocean sustainability science. Mar Ecol Prog Ser 663:1–29

Plumlee JD, Wells RJD (2016) Feeding ecology of three coastal shark species in the northwest Gulf of Mexico. Mar Ecol Prog Ser 550:163–174

Poiesz SSH, Witte JIJ, van der Veer HW (2020) Only a few key prey species fuel a temperate coastal fish food web. Mar Ecol Prog Ser 653:153–166

Queiroz N, Humphries NE, Mucientes G, Hammerschlag N and others (2016) Ocean-wide tracking of pelagic sharks reveals extent of overlap with longline fishing hotspots. Proc Natl Acad Sci USA 113:1582–1587

R Core Team (2018) R: a language and environment for statistical computing. R Foundation for Statistical Computing, Vienna

Rabalais N, Diaz RJ, Levin L, Turner R, Gilbert D, Zhang J

(2010) Dynamics and distribution of natural and human-caused hypoxia. Biogeosciences 7:585–619

Rester JK (ed) (2017) SEAMAP environmental and biological atlas of the Gulf of Mexico, 2015. No. 263. Gulf States Marine Fisheries Commission. https://www.gsmfc.org/publications/GSMFC%20Number%20263.pdf

Rezak R, Bright TJ, McGrail DW (1985) Reefs and banks of the northwestern Gulf of Mexico: their geological, biological, and physical dynamics. Wiley, New York, NY

Robbins LL, Hansen ME, Raabe EA, Knorr PO, Browne J (2007) Cartographic production for the Florida Shelf Habitat (FLaSH) Map Study: generation of surface grids, contours, and KMZ files. Open-File Rep 2007-1397. US Geological Survey, St Petersburg, FL. https://pubs.usgs.gov/of/2007/1397/html/report.html (accessed 8 Apr 2018)

Roberts JJ, Best BD, Dunn DC, Treml EA, Halpin PN (2010) Marine Geospatial Ecology Tools: an integrated framework for ecological geoprocessing with ArcGIS, Python, R, MATLAB, and C++. Environ Model Softw 25: 1197–1207

Robinson KL, Ruzicka JJ, Hernandez FJ, Graham WM, Decker MB, Brodeur RD, Sutor M (2015) Evaluating energy flows through jellyfish and gulf menhaden (*Brevoortia patronus*) and the effects of fishing on the northern Gulf of Mexico ecosystem. ICES J Mar Sci 72: 2301–2312

Robinson LM, Elith J, Hobday AJ, Pearson RG, Kendall BE, Possingham HP, Richardson AJ (2011) Pushing the limits in marine species distribution modelling: lessons from the land present challenges and opportunities. Glob Ecol Biogeogr 20:789–802

Robinson NM, Nelson WA, Costello MJ, Sutherland JE, Lundquist CJ (2017) A systematic review of marine-based species distribution models (SDMs) with recommendations for best practice. Front Mar Sci 4:421

Rozas LP, Minello TJ (2015) Small-scale nekton density and growth patterns across a saltmarsh landscape in Barataria Bay, Louisiana. Estuaries Coasts 38:2000–2018

Rozas LP, Minello TJ, Zimmerman RJ, Caldwell P (2007) Nekton populations, long-term wetland loss, and the effect of recent habitat restoration in Galveston Bay, Texas, USA. Mar Ecol Prog Ser 344:119–130

Santora JA, Schroeder ID, Field JC, Wells BK, Sydeman WJ (2014) Spatio-temporal dynamics of ocean conditions and forage taxa reveal regional structuring of seabird–prey relationships. Ecol Appl 24:1730–1747

Scales KL, Miller PI, Hawkes LA, Ingram SN, Sims DW, Votier SC (2014) On the front line: frontal zones as priority at-sea conservation areas for mobile marine vertebrates. J Appl Ecol 51:1575–1583

Sheaves M (2009) Consequences of ecological connectivity: the coastal ecosystem mosaic. Mar Ecol Prog Ser 391: 107–115

Shipp RL, Bortone SA (2009) A perspective of the importance of artificial habitat on the management of red snapper in the Gulf of Mexico. Rev Fish Sci 17:41–47

Sievers M, Brown CJ, Tulloch VJD, Pearson RM, Haig JA, Turschwell MP, Connolly RM (2019) The role of vegetated coastal wetlands for marine megafauna conservation. Trends Ecol Evol 34:807–817

Spaet JLY, Manica A, Brand CP, Gallen C, Butcher PA (2020) Environmental conditions are poor predictors of immature white shark *Carcharodon carcharias* occurrences on coastal beaches of eastern Australia. Mar Ecol Prog Ser 653:167–179

Spies RB, Senner SE, Robbins CS (2016) An overview of the northern Gulf of Mexico ecosystem. Gulf Mex Sci 1: 98–121

Story M, Congalton RG (1986) Accuracy assessment: a user's perspective. Photogramm Eng Remote Sensing 52:397–399

Sundblad G, Bergström U, Sandström A, Eklöv P (2014) Nursery habitat availability limits adult stock sizes of predatory coastal fish. ICES J Mar Sci 71:672–680

Swets JA (1988) Measuring the accuracy of diagnostic systems. Science 240:1285–1293

Switzer TS, Chesney EJ, Baltz DM (2015) Habitat use by juvenile red snapper in the northern Gulf of Mexico: ontogeny, seasonality, and the effects of hypoxia. Trans Am Fish Soc 144:300–314

Szedlmayer ST, Lee JD (2004) Diet shifts of juvenile red snapper (*Lutjanus campechanus*) with changes in habitat and fish size. Fish Bull 102:366–375

Tarnecki JH, Wallace AA, Simons JD, Ainsworth CH (2016) Progression of a Gulf of Mexico food web supporting Atlantis ecosystem model development. Fish Res 179: 237–250

US Fish and Wildlife Service (2018) National wetlands inventory. www.fws.gov/wetlands/ (accessed 11 Dec 2018)

Walbridge S, Slocum N, Pobuda M, Wright DJ (2018) Unified geomorphological analysis workflows with Benthic Terrain Modeler. Geosciences 8:94

Wannamaker CM, Rice JA (2000) Effects of hypoxia on movements and behavior of selected estuarine organisms from the southeastern United States. J Exp Mar Biol Ecol 249:145–163

Wells RJD, Cowan JH Jr, Fry B (2008) Feeding ecology of red snapper *Lutjanus campechanus* in the northern Gulf of Mexico. Mar Ecol Prog Ser 361:213–225

Wentworth CK (1922) A scale of grade and class terms for clastic sediments. J Geol 30:377–392

Williams SJ, Flocks J, Jenkins C, Khalil S, Moya J (2012) Offshore sediment character and sand resource assessment of the northern Gulf of Mexico, Florida to Texas. J Coast Res 60:30–44

Wisz MS, Pottier J, Kissling WD, Pellissier L and others (2013) The role of biotic interactions in shaping distributions and realised assemblages of species: implications for species distribution modelling. Biol Rev Camb Philos Soc 88:15–30

Zuercher R, Galloway AWE (2019) Coastal marine ecosystem connectivity: pelagic ocean to kelp forest subsidies. Ecosphere 10:e02602

Editorial responsibility: Simon Pittman, Oxford, UK
Reviewed by: M. Sievers, D. Haulsee and 1 anonymous referee

Submitted: May 11, 2021
Accepted: October 8, 2021
Proofs received from author(s): December 22, 2021